GONÇALO DOS SANTOS AFONSO

BSc in Biology

Zap1 is required for *Candida glabrata* response to fluconazole

GONÇALO DOS SANTOS AFONSO

BSc in Biology

Zap1 is required for *Candida glabrata* response to fluconazole

Zap1 is required for *Candida glabrata* response to fluconazole

Gonçalo dos Santos Afonso

Licenciado em Biologia

Orientador:	Catarina Pimentel, Investigadora Auxiliar, Instituto de Tecnologia Química e Biológica António Xavier
Coorientador:	Sofia Silva, Investigadora, Instituto de Tecnologia Química e Biológica António Xavier

Júri:

Presidente:	Rita Sobral, Professora Auxiliar, NOVA School of Science and Technology
Arguente:	Regina Menezes Echaniz, Professora Auxiliar, Universidade Lusófona de Humanidades e Tecnologias/Escola de Ciências e Tecnologias da Saúde
Orientador:	Catarina Pimentel, Investigadora Auxiliar, Instituto de Tecnologia Química e Biológica António Xavier

MESTRADO EM MICROBIOLOGIA MÉDICA

Universidade NOVA de Lisboa
Novembro, 2021

Zap1 is required for *Candida glabrata* response to fluconazole

Acknowledgments

This phase of my life was only possible to achieve due to the support, affection, dedication and help from several people, that I have the pleasure to have by my side, to whom I express my sincere gratitude.

Firstly, I would like to express my gratitude to my supervisor, Dr. Catarina Pimentel, and to my co-supervisor, Dr. Sofia Silva, for giving me the opportunity to work in such amazing environment and specially for always being available to help and guide me through this journey.

To Dr. Catarina Amaral and my lab colleagues, Andreia, Carolina and Cláudia, for always providing a good working environment and for all the support and patience through all the failed experiments.

To my true friends for their affection, patience, and support in the good and bad days throughout all these years we have been together.

To my family, for their support and sacrifices made over the years, encouraging, and believing in me and in my potential to achieve everything and anything I wish.

Lastly, I want to thank to Ana Catarina, without her a lot of my achievements would not be possible. Thank you for standing by my side even through the hardest days and being the awesome person, you are.

Abstract

Invasive fungal infections are a major healthcare problem. In these diseases, the fungus enters the bloodstream and can affect any organ, causing serious hard-to-treat infections that are associated with high mortality rates. The first line of treatment for many invasive fungal infections is fluconazole, the most prescribed antifungal drug in the world. However, the fungistatic, rather than fungicidal, nature of this drug has fostered the emergence of resistant clinical isolates. To overcome this problem, great efforts have been made to fully understand the fungal response to fluconazole.

In this work, we show that in *Candida glabrata,* one of the most prevalent fungal species causing nosocomial invasive infections*,* the transcription factor Zap1 is important for yeast growth under zinc-limited conditions. We also demonstrate that Zap1 down-regulates biofilm formation. Moreover, in line with our group's previous work, showing that deletion of *ZAP1* renders cells more sensitive to fluconazole, we found that the mutant *CgΔzap1* accumulates higher levels of fluconazole, which correlates well with its lower levels of ergosterol. Surprisingly, we observed that Zap1 is a negative regulator of the drug efflux transporter gene *CDR1* and of its regulator, *PDR1*. The apparent paradox of drug accumulation in cells where genes encoding transporters relevant for drug extrusion are being overexpressed, led us to test if their activity could be impaired. Our results indicate that Zap1-depleted cells present, in addition to decreased ergosterol levels, altered composition of membrane phospholipids, which together should impact membrane function and therefore prevent fluconazole detoxification.

Overall, this study brings to light the multifaceted transcription factor Zap1 as an important hub in *Candida glabrata* response to zinc deficiency, biofilm formation and fluconazole detoxification.

Keywords: Zap1, fluconazole, drug efflux, Cdr1, Pdr1, zinc

Resumo

As infeções fúngicas invasivas são um problema de saúde preocupante, principalmente no meio hospitalar. Nestas doenças infeciosas, o fungo entra na corrente sanguínea e pode afetar qualquer órgão. Sendo infeções graves e de difícil tratamento que estão geralmente associadas a elevadas taxas de mortalidade. O tratamento de primeira linha para as infeções fúngicas invasivas é o fluconazol, um dos antifúngico mais prescrito mundialmente. No entanto, a sua natureza fungistática, em vez de fungicida, tem favorecido o aparecimento de isolados clínicos resistentes. De forma a superar este problema, têm sido envidados grandes esforços para compreender a resposta dos fungos ao fluconazol.

Neste trabalho mostramos que, em *Candida glabrata,* uma das espécies fúngicas mais prevalentes em infeções invasivas nosocomiais, o fator de transcrição Zap1 é necessário para o seu crescimento em condições de deficiência de zinco. Demonstramos também que Zap1 é um regulador negativo da formação de biofilmes. Corroborando trabalhos anteriores do nosso grupo, onde se observou que a deleção de *ZAP1* torna as células mais sensíveis ao fluconazol, verificámos ainda que o mutante *CgΔzap1* acumula mais fluconazol e apresenta níveis menores de ergosterol. Surpreendentemente, observámos que Zap1 é um regulador negativo do transportador de efluxo de drogas *CDR1* e do seu regulador, *PDR1*. O aparente paradoxo da acumulação da droga em células onde transportadores relevantes para a sua extrusão estão a ser sobrexpressos, levou-nos a considerar que a atividade destes poderia estar afectada. Corroborando esta hipótese, constatámos que células sem Zap1 apresentam, além da diminuição dos níveis de ergosterol, uma composição de fosfolipídios membranares alterada que, em conjunto, poderão afetar a função da membrana prejudicando a desintoxicação de fluconazol.

Em suma, provamos que, em *Candida glabrata,* o fator de transcrição Zap1 é um regulador multifacetado, cuja função engloba a adaptação à deficiência de zinco, formação de biofilmes e desintoxicação de fluconazol.

Palavras-chave: Zap1, fluconazol, efluxo de drogas, Cdr1, Pdr1, zinco

Index

Tables Index

Abbreviations

XVII

CFU – Colony Formation Units

DMEM – Dulbecco's modified Eagles's medium

DMSO – Dimethyl sulfoxide

FBS – Fetal bovine serum

Fluc – Fluconazole

IC – Invasive Candidiasis

ICU – Intensive Care Unit

IFI – Invasive Fungal Infections

MOI – Multiplicity of infection

OD – Optical density

PAMP – Pathogen Associated Molecular Patterns

PBS – Phosphate-buffered saline

PI – Propidium iodide

R6G – Rhodamine 6G

SC – Complete Synthetic Medium

SD – Standard Deviation

Sod – Superoxide dismutase

TLR2 – Toll-like receptor 2

TLR4 – Toll-like receptor 4

IFN-γ – Interferon gamma

YPD – Yeast Extract Peptone Dextrose media

Zn – Zinc

Chapter 1 – Introduction

1.1 Fungi and fungal infections

Fungi are a heterogeneous group of organisms that, unlike other eukaryotes, are composed of cells containing (i) a cell wall with chitin and glucans in its structure; and (ii) ergosterol instead of cholesterol, as the main sterol of cellular membranes (*1*). They range from unicellular organism, like yeasts, to multicellular organisms like molds and mushrooms. Yeasts are commonly round or elliptical organisms that can reproduce asexually via fission or budding. Molds are multicellular organisms, composed of hyphae that, regardless of their sexual stage, always reproduce through very resistant spores capable of being widely and easily dispersed.

Fungi can be found almost anywhere in the environment, very often in association with plants and animals. Some fungi are commensals of humans and are mainly found in the mucosal surfaces (*1, 2*). Human commensal fungi comprise more than 50 genera of fungi, including *Candida*, *Saccharomyces*, and *Cladosporium,* which appear predominantly in the gut, while *Malassezia*, *Aspergillus* and *Penicillium* are usually found in the skin. Several studies suggest a vast and complex balance of microbe-to-microbe interactions within human microbiota with fungi and bacteria competing for nutrients and secreting a wide range of molecules to promote or restrict each other's growth (*3*).

Fungi can be opportunistic or primary pathogens. The former tends to cause infections in people with weakened immune system, while the latter are capable of infecting perfectly healthy individuals (*4, 5*). Fungal infections affect billions of people every year, but the global burden and epidemiology of fungal diseases is hard to estimate, due to the absence of regular surveillance systems and mandatory reporting of these diseases (*2, 4*). Fungal infections can range from superficial affecting skin, nails and mucosa surfaces to invasive where fungi enter the bloodstream and colonize host organs. Invasive fungal infections are the most life-threatening fungal diseases, being associated with high morbidity and mortality rates, and higher healthcare costs. Fungi are major pathogens of critically ill patients and nosocomial invasive fungal infections currently represent 10% of all hospital acquired infections (*4, 6*).

Most invasive fungal infections are caused by *Aspergillus*, *Candida* and *Cryptococcus* species. Other fungi such as *Pneumocystis jirovecii, Histoplasma capsulatum* and Mucormycetes, although less frequent, are also responsible for severe diseases (*4, 7*). *Candida albicans* is also the main agent responsible for mucosal disease, *Aspergillus fumigatus* for most allergic fungal disease and *Trichophyton rubrum*, for skin infections (*4, 7*).

1.2 *Candida* infections

Candida species are commensals of humans, and colonize asymptomatically skin and mucosal surfaces such as the oral and vaginal cavity, and the gastrointestinal tract of most healthy individuals (*7*). However, *Candida* spp. can easily switch from a commensal to a pathogenic state due to several risk factors. Among them is the use of broad-spectrum antibiotics that suppress the growth of normal bacterial flora and increase *Candida* spp. colonization. The list of risk factors also includes parenteral nutrition, disruption of the mucosal barriers, gastrointestinal or cardiac surgery, prolonged hospital and intensive care unit (ICU) stays, premature neonate and immunosuppression states such as neutropenia, chemotherapy, corticosteroid therapy and HIV infection (*8, 9*).

Candida infections, or candidiasis, range from mucocutaneus or cutaneous to invasive, in which internal organs are affected. Invasive candidiasis is the most severe and life-threatening type of *Candida* infection, and often manifests in the form of candidemia, which occurs when the fungus enters the bloodstream. The disease is usually triggered by the disruption of physical barriers, such as the epithelium and the normal mucosal, increased adhesion and proliferation of *Candida spp.* and malfunctioning of the immune system (*10, 11*).

Timely diagnosis of Candidiasis is difficult because the clinical symptoms are not specific and therefore the disease is frequently misdiagnosed. On the other hand, current diagnostic tools, heavily rooted in microscopy or microbiological cultures, lack sensitivity (may lose more than 50% of candidemias) and take too long to deliver results (*12*).

Only a minority of *Candida* species has been reported to infect humans, since 65% of them are unable to grow at a temperature of 37 ºC (*10*). *Candida albicans* is the *Candida* species that most causes invasive nosocomial infections, around 57% of all cases (Fig. 1.1), according to the data from the EUROBACT study (*6, 8, 13, 14*). However, over the last years there has been an epidemiologic shift and non-*albicans* species have increased their prevalence (*15, 16*). Among non-*albicans* species, *Candida glabrata* is the most prevalent being responsible for 15-25% of all nosocomial invasive candidiasis cases (*8, 15, 16*).
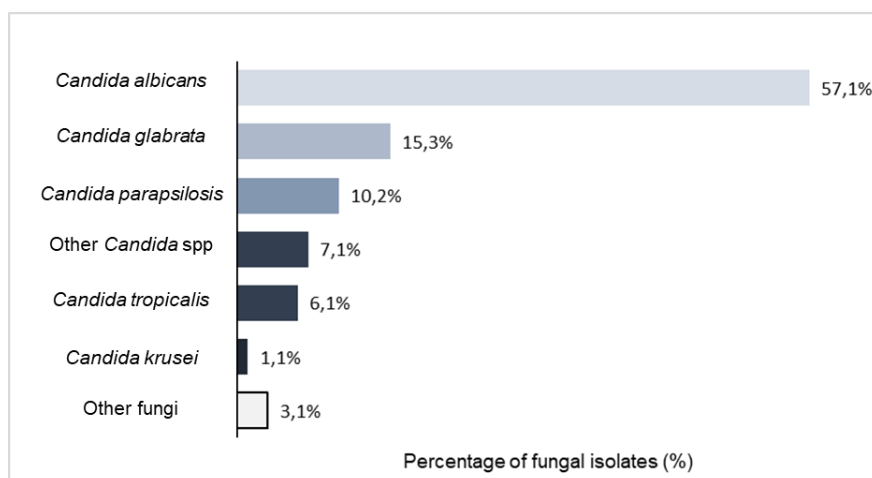
Figure 1.1: **Epidemiology of invasive *Candida* infections** (Adapted from José-Artur Paiva et al. Critical Care, 2016).

1.3 *Candida glabrata*

C. glabrata is an asexual, haploid yeast (contrary to *C. albicans* that has a diploid genome) and nondimorphic, forming small blastoconidia under all environmental conditions. As a pathogen, it is the only *Candida* species that does not form pseudohyphae at temperatures above 37°C. Pseudohyphae are a chain off cells formed by newly-dividing cells through budding where the buds do not separate (*17*). *C. glabrata* is phylogenetically closer to the model yeast *Saccharomyces cerevisiae* than to *C. albicans* (*18, 19*). *C. glabrata* was first classified in the *Torulopsis* genus due to its lack of pseudohyphae. Later, it was considered that the ability to form pseudohyphae was not a trustworthy distinctive aspect for members of the genus *Candida* and it was suggested *Torulopsis glabrata* to be classified in the genus *Candida*, because of its human pathogenicity (*19, 20*). On the selective medium Chromagar, a medium capable of distinguish several *Candida* species based on the colors of the forming colonies, *C. glabrata* colonies range from pink to purple and *C. albicans* colonies from blue-green to green.

C. glabrata like other *Candida* species commensally colonize oral and gut mucosal surfaces. The risk factors for *C. glabrata* infection include prolonged hospitalization, prior antibiotic use, hand carriage by hospital personnel and use of fluconazole (*19*). The mortality rate associated with *C. glabrata* infections, falling in the range of 40% to 70%, is one of the highest among nosocomial invasive candidiasis (*21*).

C. glabrata has several virulence factors that make it a human pathogen (Fig. 1.2). Among them is the secretion of hydrolytic enzymes that destroy host tissues to surpass the mucosal surface, and the secretion of phospholipases that induce damage of the host cell membrane to expose the receptors that facilitate adherence. *C. glabrata* also produces lipases and hemolysins that hydrolyze triacylglycerols and can degrade hemoglobin, respectively. The latter is thought to be a mechanism used by the yeast to obtain iron for its metabolic processes. This mechanism is, however, poorly understood because *C. glabrata* cannot efficiently use hemoglobin as the only source of iron (*20, 22*). Unlike *C. albicans*, *C. glabrata* does not produce significant levels of extracellular proteinase activity (*23*).

Another important virulence factor of *C. glabrata* is its ability to adhere to host cells and form biofilms. *C. glabrata* is capable of colonizing host tissues as well as abiotic surfaces where it develops as a multilayered biofilm structure. Biofilms are surface-attached and structured microorganism communities embedded in a self-produced extracellular matrix composed of proteins, carbohydrates, and other components. The biofilm structure protects fungal cells from the host immune system and from antifungal drugs, which have a low ability to penetrate in the extracellular matrix (*20, 24-26*). The *Epa* (epithelial adhesin) gene family encodes a major group of proteins, adhesins, responsible for adhesion during biofilm formation. For example, the gene *EPA1* is needed for *in vitro* adhesion while, *EPA6* and *EPA7* gene are expressed during urinary tract infection and biofilm formation (*20, 27*). The ability to form biofilms contributes to the survival of *C. glabrata* as a commensal and pathogen,

allowing them to evade the host immune mechanisms, resist antifungal treatment, and withstand the competitive pressure from other microorganisms.

The genomic plasticity of *C. glabrata* is also a key factor for its virulence, which allows the yeast to rapidly adapt to a multitude of hostile host and environmental conditions. Indeed, several clinical isolates present marked differences in their genome organization due to chromosomal rearrangements, translocations, chromosome fusions and inter-chromosomal duplications as well as *de novo* chromosome generation (*28*).
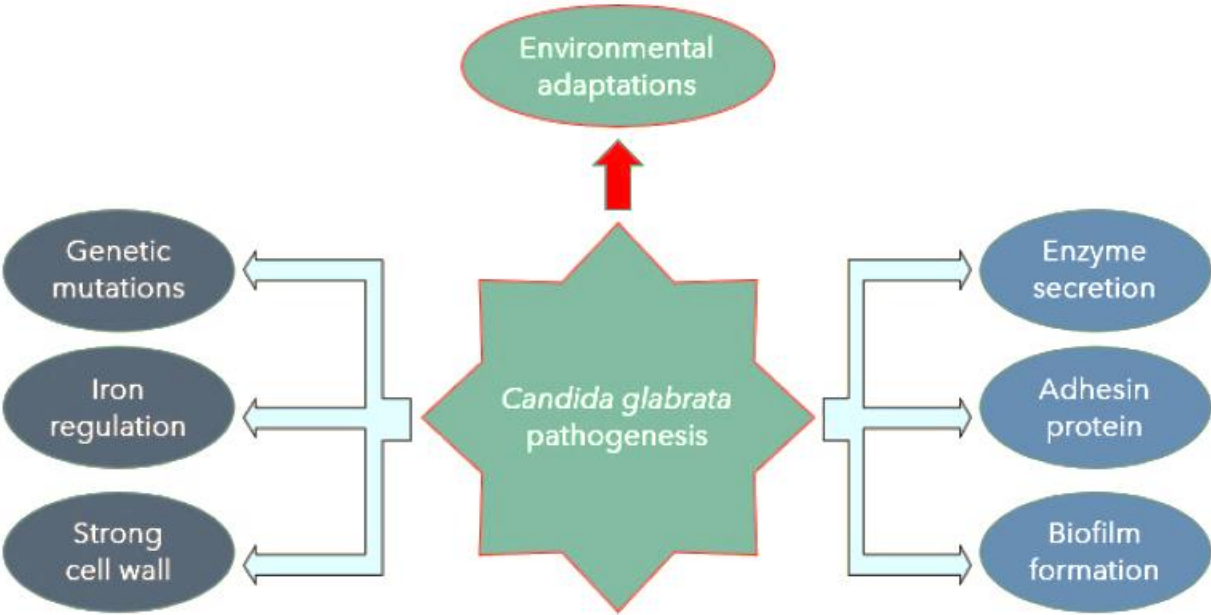
Figure 1.2: ***Candida glabrata* pathogenesis mediated by virulence factors**. (Adapted from Hassan, Y., S.Y. Chew, and L.T.L. Than, *Candida glabrata*: Pathogenicity and Resistance Mechanisms for Adaptation and Survival. J Fungi (Basel), 2021. 7(8).).

1.4 *Candida glabrata*-host interactions

The immune system surveys commensal microorganisms, guarantying that they do not turn into pathogens. The first line of defense of the host immune system is the innate immunity, which relies on physical barriers, such as skin and mucous membranes. Once fungi transpose these physical barriers, phagocytes, such as macrophages, neutrophils and dendritic cells, respond to the infection site and play an essential role trying to stop the infection progress. Cells from the innate immune system are able to rapidly recognize microbial infection through Pattern Recognition Receptors (PRRs). The PRRs recognize a group of conserved molecular patterns common to large groups of microbial species, the Pathogen-Associated Molecular Patterns (PAMPs). The recognition of PAMPs leads to the production of inflammatory mediators that promote phagocyte recruitment and stimulate phagocytic activities, antigen uptake and antigen presentation. On the other hand, during adaptive immune response to fungi there is the production of antibodies that prevent adherence, neutralize toxins, cause opsonization and antibody-dependent cellular cytotoxicity. Both innate and adaptive immunity work together as a whole to fight infections and maintain host and commensals coexistence (*29-31*).

When *C. glabrata* reaches the physiological barriers and starts its pathogenic route, the innate immune system responds. The recognition of fungi PAMPs by macrophage is made by Toll-like receptor 2 (TLR2) and Toll-like receptor 4 (TLR4) (*32*). After recognition, a cascade of intracellular signaling pathways is activated leading to reorganization of the macrophage's actin cytoskeleton and consequently to phagocytosis. After the internalization of the fungal pathogen the phagosome proceeds is maturation, fusing with lysosome and giving rise to phagolysosomes. The phagolysosome internal environment is extremely hostile to the invading pathogen due to acidification and accumulation of hydrolytic enzymes and potent reactive oxygen and nitrogen species. Macrophages also deprive the cells of nutrients and carbon sources and can also intoxicate the pathogen with copper and zinc, increasing the concentration of these metals in the phagolysosome. Although copper and zinc are essential micronutrients needed for the growth of all organisms, such a burst negatively impacts the uptake of other key trace metals and affects enzymes, altering or inhibiting their activities (*33-35*).

To surpass the host defenses *C. glabrata* uses several strategies (Fig. 1.2). In fact, evasion from the host defenses is considered a central aspect of *C. glabrata* virulence. To avoid recognition by the host's immune system, *C. glabrata* resorts to cell wall remodeling, although the mechanisms underlying this phenomenon remain unclear (*36*). Another strategy is to hide the PAMPs, covering them behind a mannan layer, thus preventing macrophage recognition and activation, and consequently diminishing the inflammatory response.

C. glabrata is also capable to neutralize the antimicrobial environment in the phagosome/phagolysosome. It was shown that in the absence of glucose, *C. glabrata* metabolizes amino acids and alkalinizes the phagolysosome medium, avoiding its maturation and consequent acidification (*37*). Moreover, in order to counteract the production of reactive oxygen species (ROS),

which is one of the main mechanisms of the macrophage anti-microbial response, *C. glabrata* expresses a highly active catalase, Cta1 (*33*).

Once inside the macrophage *C. glabrata* must adapt the metabolism in order to sustain the deprivations imposed, the carbon source availability and the lack of nitrogen and other nutrients. To overcome the lack of nitrogen yeasts, downregulate protein synthesis, upregulate amino acid biosynthetic pathways and amino acid and ammonium transport genes. As an alternative carbon source, yeast cells degrade fatty acids and use lipids but can also rely on autophagy. The remodeling of chromatin plays a central role in reprograming the cellular energy metabolism inside the phagosome. And, as the macrophage imposes iron depletion, *C. glabrata* expresses, high-affinity iron transporters to increase iron uptake. (*33*).

C. glabrata is able to survive from two to three days inside the macrophage, without causing severe damage or inducing apoptosis. After *C. glabrata* phagocytosis, the macrophage produces low immunomodulating agents, which, among other functions, are responsible for macrophage recruitment. However, the high capacity of the yeast to survive and replicate within macrophages, has led several authors to propose that macrophage recruitment could be beneficial for *C. glabrata* to escape the immune system and be able cross biological barriers (*33*).

Apart from its great ability to deceive the immune system *C. glabrata* has also an inherent tolerance to currently used azole antifungals and can easily acquire mutations that make it resistant to other classes of drugs (*24, 25*).

The reasons mentioned above, together with the high prevalence of *C. glabrata* among invasive candidiasis (Fig. 1.3), have put the spotlight on this yeast, which is currently considered a major global health concern (*16*).

Figure 1.3: Global percentages of *Candida glabrata* isolates among bloodstream samples of patients with invasive candidiasis. (Adapted from: Arendrup MC. 2014. Update on antifungal resistance in *Aspergillus* and *Candida*. Clin Microbiol Infect 20 Suppl 6:42-8.)

1.5 Antifungal drugs

There are four main classes of antifungal drugs in use to treat invasive candidiasis: polyenes, antimetabolites, echinocandins and azoles, which have distinct mechanisms of action (Fig. 1.4).
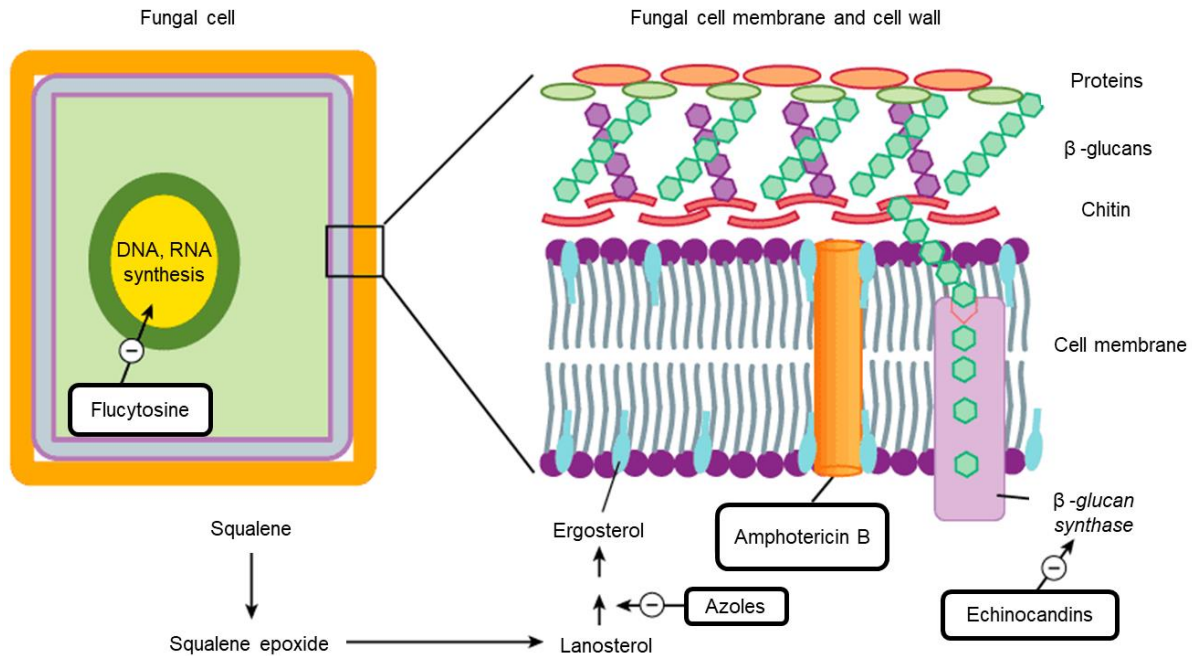
Figure 1.4: Antifungals used in the treatment of invasive candidiasis (Adapted from https://microbiologyinfo.com/mode-action-antifungal-drugs/).

Polyenes, like amphotericin B, binds to ergosterol forming pores that cause leakage of monovalent ions such as K^+, Na^+, H^+ and Cl^- and some intracellular contents causing subsequent cell death (*38*). These drugs have an affinity to cholesterol and are nephrotoxic; therefore, they are not used regularly.

The antimetabolite 5-Fluorocytosine (5-FC) is a synthetic analogue of cytosine. It enters the fungal cell via a cytosine permease. Inside the cell it is first converted into 5-fluorouracil (5-FU) and then into 5-fluorouridylic acid, which competes with uracil for the synthesis of RNA. Besides, 5-fluorouracil can be metabolized to the 5-fluorodeoxyuridine monophosphate. This compound inhibits the primary source of thymidine in DNA biosynthesis, thymidylate synthetase, due to the enzyme's inability to remove the fluorine atom (*39*).

Echinocandins, such as caspofungin, inhibit the synthesis of β-glucans, key components of the fungi cell wall, *via* noncompetitive inhibition of the enzyme Fks(1/2) 1,3-β glucan synthase, which results in the disruption of the integrity of the cell wall and leads to cell death (*40*).

Azoles are divided into two groups: imidazoles (clotrimazole, miconazole and ketoconazole) and triazoles (itraconazole, fluconazole, voriconazole, posaconazole, isavuconazole and

eficoconazole) (*41-43*). Imidazoles were the first developed azoles, but have high toxicity, severe side effects and interact with other drugs, leading them to be replaced by triazoles, which have a broader antifungal activity and increased safety profile. Thus, imidazoles are mostly used to treat superficial and mucosal infections, while triazoles are mostly used to treat systemic infections (*43*). Azoles bind to the heme cofactor of the enzyme lanosterol 14-α-demethylase (Erg11) and inhibit the biosynthesis of ergosterol (Fig. 1.5) (*44*).
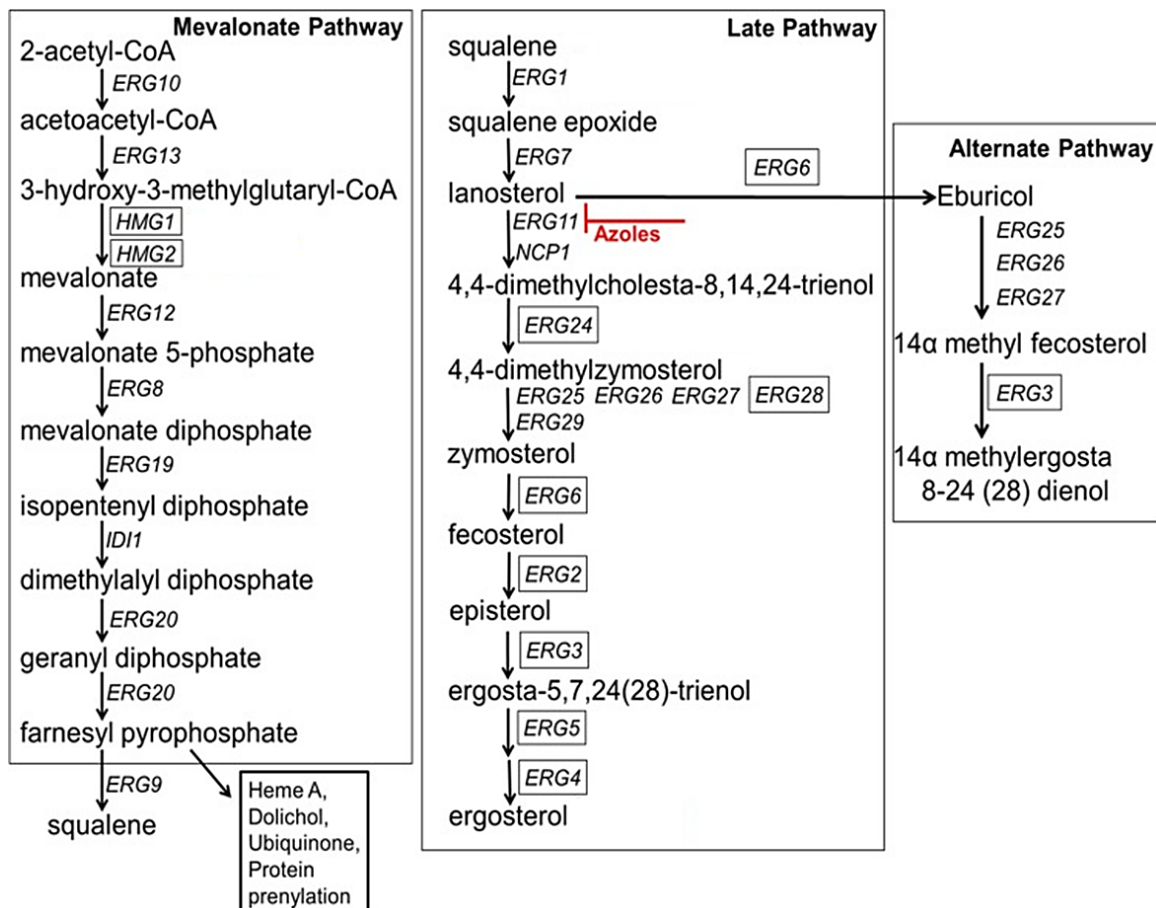
Figure 1.5: Ergosterol biosynthetic pathway (Adapted from S. Bhattacharya, B. D. Esquivel, T. C. C. P. White, Overexpression or Deletion of Ergosterol Biosynthesis Genes Alters Doubling Time, Response to Stress Agents, and Drug Susceptibility in. mBio 9, (2018).).

The azole fluconazole is the most prescribed antifungal agent and the frontline drug used in the prophylaxis and treatment of several fungal infections (*45-47*). The inhibition of 14α-demethylase leads to depletion of ergosterol and accumulation of sterol precursors, including 14α-methylated (Fig. 1.5) sterols, resulting in a change of membrane fluidity and function that impairs vital processes, such as signaling, transport, exocytosis and endocytosis, and also prevents growth and cell division (*48*).

According to European guidelines, the first line of treatment for invasive candidiasis is fluconazole and/or echinocandins. Amphotericin B and other azoles are alternatively used in case the infection does not respond to the first line treatments.

1.6 Antifungal drug resistance in *Candida glabrata*

C. glabrata infections pose a serious problem due to their inherent and acquired resistance to antifungal drugs currently in use (*20*) (Fig. 1.6). With regard to echinocandins, which inhibit Fks(1/2) 1,3-β-D-glucan synthase, resistance to this antifungal drug has been reported and believed to be associated with prior echinocandin exposure that promotes the occurrence of mutations in the β-(1,3)-D-glucan synthase *FKS* subunits genes, decreasing the interaction with the drug (*20, 27, 49-51*).

Decreased susceptibility to polyenes has also been reported in *C. glabrata*. The phenotype appears to correlate with a reduction in ergosterol content in the plasma membrane (*49, 52*).

C. glabrata has an inherent tolerance to azoles, such as fluconazole. The low susceptibility to fluconazole could potentially be due to the ability of this yeast to uptake exogenous sterols, which was observed under both aerobic and anaerobic conditions (*49, 53*). In anaerobic conditions ergosterol uptake has been linked to CgAus1, a transporter only identified in *C. glabrata* and, known to be regulated by CgUpc2, a transcription factor that has a role in sterol metabolism and is activated under low oxygen levels (*54*). It was shown that CgAus1 transporter improves the sterol uptake *in vitro* and in *in vivo* after fluconazole treatment (*54, 55*). *C. glabrata* can easily acquire several mutations that renders it more resistant to azole drugs. Reported mutations in *ERG11* (the gene that encodes the enzyme lanosterol 14-α-demethylase) usually (i) lead to a protein (Erg11) with lower azole binding ability or (ii) induce the overexpression of *ERG11* in order to counteract its inhibition by azoles (*24*). However, in *C. glabrata*, the main mechanism of resistance to azoles relies on the occurrence of genetic mutations that lead to an upregulation of the multidrug efflux transporters and consequently an increase in drug efflux. This process is commonly mediated by ATP-Binding Cassette (ABC) transporters such as Cdr1 and Cdr2, which are often associated with azole resistance. Their expression is regulated at the transcriptional level by the zinc finger transcription factor Pdr1. Gain of function (GOF) mutations in the *PDR1* gene lead to an overexpression of efflux pumps and, consequently, to an increased efflux of azoles (as well as 5-Fluorocytosine). These GOF mutations in *PDR1* also promote the ability of *C. glabrata* to adhere to host cells, which increases its virulence (*24, 27, 49, 53, 56-60*). ABC proteins may transport different azole drugs and therefore their overexpression leads to cross-resistance between azoles (*60*).

The worldwide use of azole antifungals in empiric and prophylactic treatment programs fostered the emergence of resistance (*13, 61*). The use of certain azole drugs, such as fluconazole, is appealing due to its safety profile, easy oral administration and availability in low-income countries (*47, 62*). As such, strategies that on the one hand improve fluconazole efficacy, and on the other hand avoid the emergence of resistance mechanisms, are urgently needed to preserve the use of this drug.

In our laboratory it was recently showed that following the exposure to fluconazole, *C. glabrata* downregulates the expression of *ZAP1* gene and the deletion of this gene makes yeast cells more sensitive to fluconazole (Gaspar-Cordeiro *et al.*, manuscript under review). In this sense, Zap1 opens up new possibilities in the field of fluconazole tolerance worth to be explored.
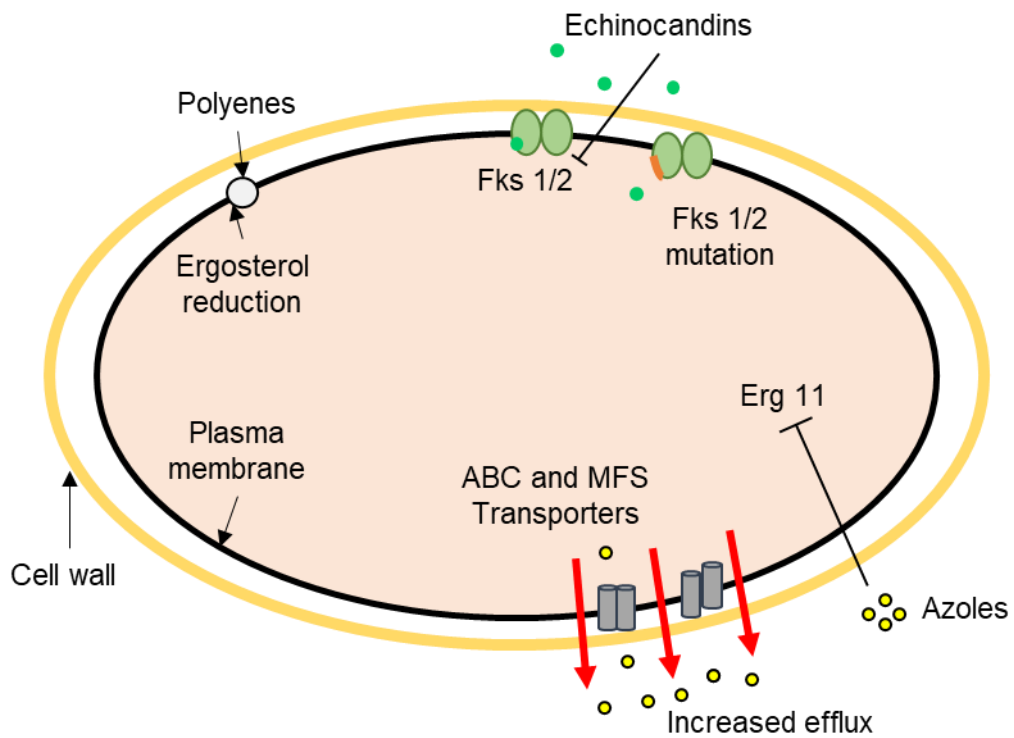
Figure 1.6: Antifungal drug resistance mechanisms in *Candida glabrata*. (Adapted from M. Tscherner, T. Schwarzmüller, K. Kuchler, Pathogenesis and Antifungal Drug Resistance of the Human Fungal Pathogen *Candida glabrata. Pharmaceuticals* **4**, 169-186 (2011).

1.7 The transcription factor Zap1

In *C. glabrata, ZAP1* is not characterized, but orthologs of the gene have been studied in several other yeast species (*63-67*). Zap1 is a transcription factor responsible for maintaining zinc homeostasis and it is capable of autoregulation. It contains two independent activation domains, AD1 and AD2, that mediate the induction of target genes. AD1 is essential to control the zinc-responsive activity of Zap1, whereas AD2 appears to play a more important role when zinc depletion is combined with other types of stresses (*68*) (Fig. 1.7).

Zinc is a fundamental micronutrient for all organisms, being an essential cofactor for several enzymes and transcription factors. Nevertheless, when present in excess it becomes toxic creating an imbalance in the cellular oxidative metabolism. The tight regulation of intracellular zinc levels is, therefore, a basic cellular process that occurs in all eukaryotic cells. Zinc also plays a role in fungal virulence as a cofactor of superoxide dismutases (Sods), which are essential enzymes for ROS detoxification upon infection (*69*).

Zap1 is a nuclear resident transcription factor, and a direct sensor of cellular zinc levels. When zinc is abundant, the metal binds to amino acid residues of AD1 and AD2 and inhibits the ability of these domains to promote transcription (*63-67*). Zap1 is able to interact with several genes involved in zinc homeostasis by binding to the cis-element 5'ACCYYNAAGGT3' located in their promoter regions. When cells become zinc-limited, Zap1 activates the expression of mobilization and zinc-uptake genes, such as *ZRT1*, *ZRT2* and *ZRT3* and *ZRC1* (*64, 70*).
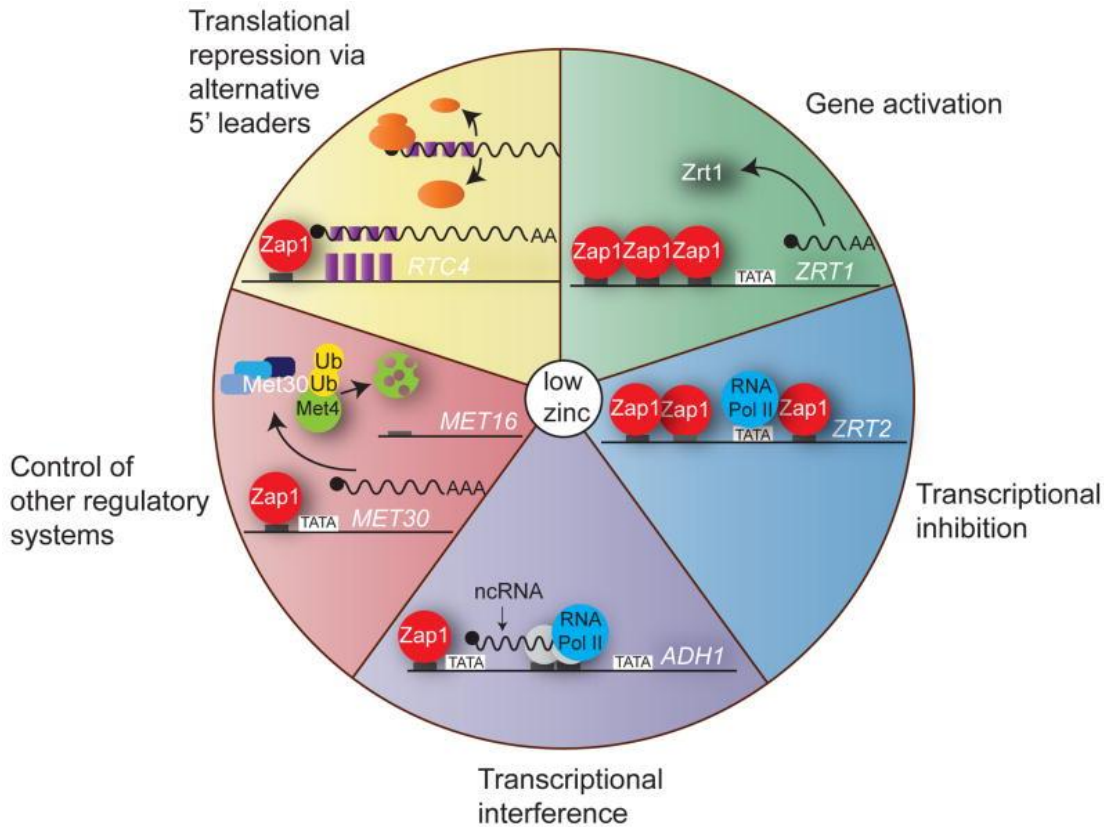
Figure 1.7: Gene regulation mechanisms of Zap1. (A. J. Bird, S. Labbé, The Zap1 transcriptional activator negatively regulates translation of the RTC4 mRNA through the use of alternative 5' transcript leaders. Mol Microbiol 106, 673-677 (2017).)

The *ZRT1* gene encodes a high affinity zinc transporter protein strongly induced under zinc depletion conditions. The *ZRT2* gene encodes a low affinity zinc transporter, which is induced by mild zinc limitation and repressed by more severe zinc deficiency. The *ZRT3* gene encodes a vacuolar membrane protein responsible for transporting zinc stored in the vacuole to the cytoplasm. The mobilization of zinc stores from the vacuole is a first-line response to zinc deprivation. *ZRC1* codes for a vacuolar membrane zinc transporter that transports zinc from cytosol to vacuole for storage. It is also induced by Zap1 durinc zinc deficiency as a protective measure; when zinc-deficient cells are re-supplied with zinc, the high activity of zinc uptake transporters results in rapid zinc overload and Zrc1 is needed to sequester the excess zinc in the vacuole (*64, 68, 71*).

Other studies revealed that Zap1 also regulates several genes encoding proteins whose activity go beyond zinc homeostasis. Zap1 is a negative regulator of genes involved in biofilm matrix formation. Zap1 binds directly to the promoter region of the *CSH1* and *IFD6* genes, which encode proteins that inhibit matrix accumulation. It also represses the expression of *GCA1*, *GCA2*, and *ADH5* genes that are known to promote matrix accumulation (*65, 72-74*) (Fig. 1.8). Moreover, Zap1 is a positive regulator of phospholipid biosynthesis. Phospholipids are amphipathic molecules and major structural components of cellular membranes, but they can also provide precursors for the synthesis of macromolecules, serve as molecular chaperones, assist protein modification for membrane

association and be reservoirs of second messengers (*75*). Phospholipids are essential for vital cellular processes. Cells depleted of zinc contain increased levels of phosphatidylinositol (PI) and decreased levels of phosphatidylethanolamine (PE) and, both phospholipids play a role in the modification of proteins for attachment to membranes. For example, PE can be used for the glycosylphosphatidylinositol modification of proteins and PI can be used for the synthesis of glycosylphosphatidylinositol anchor and for the synthesis of polyphosphoinositides and sphingolipids. Zap1 stimulates the expression of the *DPP1* and *PIS1* genes. *DPP1* codes for diacylglycerol pyrophosphate phosphatase that modifies the phopholipds of the vacuolar membrane, and *PIS1* encodes a phosphatidylinositol synthase that catalyzes the synthesis of PI. In *Saccharomyces cerevisiae* zinc-mediated regulation of phospholipid synthesis affects membrane phospholipid composition, and the main transcription factor involved in this regulation is Zap1 (*72-75*).
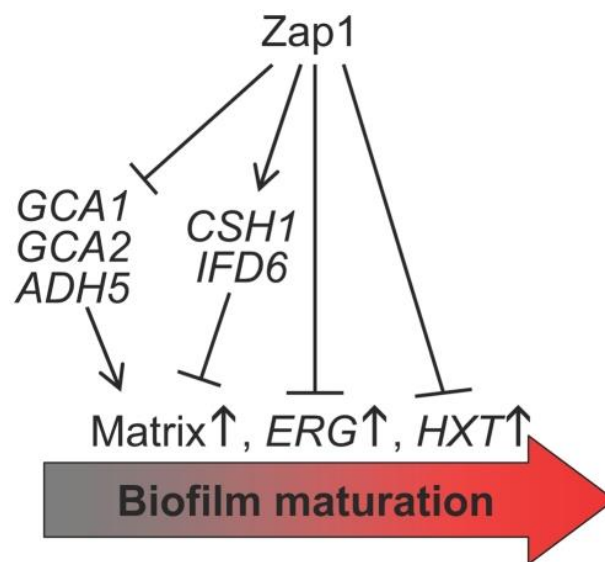
Figure 1.8: Zap1 regulates genes important for biofilm formation. (Nobile, C.J., et al., Biofilm matrix regulation by *Candida albicans* Zap1. PLoS Biol, 2009 7(6): p. e1000133).

1.8 Objectives

Invasive infections caused by *C. glabrata* are on the rise and the inherent tolerance of this species to fluconazole, a widely used drug for the treatment of candidiasis, makes this trend even more alarming. In this context, strategies to increase the efficacy of fluconazole against this species are very much needed.

Previous work from our laboratory has unveiled a link between Zap1 and fluconazole tolerance. Gaspar-Cordeiro *et al.* showed that *C. glabrata* cells depleted of Zap1 were less tolerant to fluconazole. Therefore, strategies targeting Zap1 might, in principle, improve fluconazole activity against *C. glabrata*. However, at this stage, a clear understanding of the underlying mechanisms is needed to strengthen such an approach. In this sense, the main objectives of this work are:

i) To assess whether Zap1 in *C. glabrata*, similarly to its orthologues, regulates zinc homeostasis;

ii) To understand the role of Zap1 in the *C. glabrata* response to fluconazole.

Chapter 2 – Materials and Methods

2.1 Solutions and culture media

Solutions and culture media were prepared as follows:

- Fluconazole stock solution (2.5 mg/mL) was prepared by dissolving the powder in water.
- Zinc sulfate ($ZnSO_4$) stock solution (0.144 g/L) was prepared by dissolving Zinc sulfate heptahydrate powder in water
- Synthetic complete medium (SC) pH 5.5 (Complete Supplement Mixture: 0.77 g/L (0.4mg/L $ZnSO_4$); yeast nitrogen base w/o amino acids and ammonium sulphate 1.7 g/L; ammonium sulphate 5.4 g/L; glucose 2%.
- Synthetic complete medium lacking Zinc (SC -Zn) pH 5.5 (Complete Supplement Mixture: 0.77 g/L; yeast nitrogen base w/o amino acids and $ZnSO_4$ 6.9 g/L (Formedium); glucose 2%.
- Synthetic complete medium lacking Zinc (SC +Zn) pH 5.5 (Complete Supplement Mixture: 0.77 g/L; yeast nitrogen base w/o amino acids and $ZnSO_4$ 6.9 g/L (Formedium); glucose 2%; 0.4mg/L $ZnSO_4$ Added posteriorly.
- Yeast Extract Peptone Dextrose media (YPD) (yeast extract 10 g/L; peptone 20 g/L; glucose 20 g/L; Agar 1.5%).

2.2 Strains and Culture Conditions

The strains used in this work are listed in Table 2.1. Yeast species were maintained in Yeast Extract Peptone Dextrose media (YPD) agar plates and grown at 30°C *Candida albicans* and *Saccharomyces cerevisiae* or 37°C *C. glabrata*. Unless otherwise stated, all assays were performed in synthetic complete medium (SC) pH 5.5 (Complete Supplement Mixture: 0.77 g/L; yeast nitrogen base w/o amino acids and ammonium sulphate 1.7 g/L; ammonium sulphate 5.4 g/L; glucose 2%). Yeast cultures were grown until exponential phase (OD_{600} 0.8) and treated with 32 µg/mL fluconazole for 24 h.

2.2.1 Growth curves

Growth curves with *C. glabrata* HTL (WT), Δ*zrt1* and Δ*zap1* were carried out by doing a pre-inoculum of cells grown overnight using SC medium without zinc. In the next day, cells were added to 96 well plates at 0.1 OD_{600} in 200 µL in each well. Cells were incubated for 24 h at 37 ºC in Biotek ELx808 and OD_{600} was measured every 30 min intervals. Assays were performed using biological quadruplicates.

For growth curves, *C. glabrata* Δ*zap1* transformed with pZAP1 or pCgACT14 (vector) were grown overnight in SC medium lacking tryptophan. In the next day cells were diluted to 0.1 OD_{600} in selective defective medium, lacking tryptophan and zinc (SC-Zn-TRP) and 200 μL were added to a 96 well plate. Plates were incubated for 24 h at 37 ºC in Biotek ELx808 and OD_{600} was measured every 30 min intervals. Assays were performed using biological quadruplicates.

2.2.2 Spot assays

A pre-inoculum of cells was grown overnight. In the next day these cultures were used to inoculate SC medium at OD_{600} 0.2, and fresh cultures were grown until early exponential phase (OD_{600} 0.8). Cultures were then 10-fold serial diluted and 5 μL of each dilution were spotted onto SC media agar plates supplemented or not with the indicated compounds. Plates were incubated for 24 h or 48 h at 37 ºC (*C. glabrata*), 48 h at 30 ºC (*Candida albicans*) or for 72 h at 30 ºC (*Saccharomyces cerevisiae*).

2.2.3 Microscopy

C. glabrata cells were grown until early exponential phase (OD_{600} 0.8) and treated or left untreated with fluconazole (32 μg/mL). After 24 h at 37ºC, 1mL of the cultures were centrifuged (5000g, 1 minute) and resuspended in approximately 100 μL of medium. For phase contrast microscopy 5 μL of cell suspension were spotted on 1.7% agarose coated glass slides and observed in a LeicaDM6000B. Pictures were acquired using a phase contrast objective Uplan F1 100✕ and coupled to a CCD camera Andor IxonEM (Andor Technologies) through the program Metamorph, version 5.8 (Universal Imaging).

Strain	Genotype	Source
C. glabrata HTL	his3Δ::FRT leu2Δ::FRT trp1Δ::FRT	(101)
C. glabrata ΔCAGL0E01353g	*CAGL0E01353g*::*HIS3* leu2Δ::FRT *trp1Δ*::FRT	Carmo, Beatriz. Master thesis in microbiology (2020)
C. glabrata Δzap1	*ZAP1*::his3Δ leu2Δ::FRT trp1Δ::FRT	(100)
C. albicans CJN1201 (Δ*zap1*/ Δ*zap1*)	ura3Δ::λimm434; arg4::hisG; his1::hisG::pHIS1; zap1::ARG4 ura3Δ::λimm434; arg4::hisG; his1::hisG zap1::URA3	(65)
C. albicans DAY185	ura3Δ::λimm434 ARG4:URA3::arg4::hisG his1::hisG::pHIS1 ura3Δ::λimm434 arg4::hisG his1::hisG	(102)
S. cerevisiae BY4742	MATα his3Δ1 leu2Δ0 lys2Δ0 ura3Δ0	Euroscarf
S. cerevisiae Δzap1	MATα his3Δ1 leu2Δ0 lys2Δ0 ura3Δ0 ZAP1::kanMX4	Euroscarf

2.2.4 Mutant strain complementation

C. glabrata ZAP1 gene was amplified by PCR using the primers. ZAP1_A1 and ZAP1_A4 (Table 2.2) with an annealing temperature of 58ºC for 10 seconds and an extension temperature of 72ºC for 1 minute and 30 seconds. The expected amplicon size was 2533 bp. PCR product were run in an agarose gel electrophoresis to confirm gene disruption (Fig. 7.1).

Table 2.2: Zap1 primers

Primers	Sequence
ZAP1_A1	5' AATGCAAGAGGGACAAATCG 3'
ZAP1_A4	5' GTTGATCACAGCGAGAAGC 3'

The *ZAP1* fragment was cloned into the vector pCgACT-14 encoding the β-lactamase gene, which confers resistance to ampicillin and carbenicillin, and also the *TRP1* gene, required for tryptophan biosynthesis. The plasmid (400 ng) was digested with the endonuclease *Sma*I at 25ºC for 3h, followed by inactivation of the enzyme at 65ºC for 10 minutes. Next, approximately 2000 ng of the *ZAP1* fragment were added to 10 ng of the digested plasmid and the ligation was performed using T4 DNA ligase (NEW ENGLAND BioLabs Inc.), and incubated at room temperature for 2 hours, followed by inactivation of T4 DNA ligase by incubation at 65 ºC for 10 minutes. The ligation reaction was used to transform competent *E. coli* cells (XL1 Blue). For that, 2 μL of the reaction volume was added to *E. coli* competent cells and left on ice for 30 minutes. Then, the tubes were placed on a 42ºC bath for 35 seconds, followed by a 2-minute incubation on ice. Subsequently, 800 μl of super optimal broth with catabolite repression medium (SOC: 2% bactotryptone, 0.5% yeast extract, 10 mM NaCl, 2.5mM KCl, 10 mM $MgCl_2$, 10 mM $MgSO_4$, 20 mM glucose) were added to each tube and the cells were incubated at 37ºC for 1 hour. 50 μL of cells were next plated onto LB (Luria Bertani broth) agar plates with 100 μg/mL of carbenicillin, containing IPTG (0.1 M) and X-gal (400 mM), for blue white selection. Plates were incubated for 24 h at 37ºC. The white colonies (containing the plasmid with a disrupted lacZ gene) were used to inoculate 2 mL of liquid LB containing 100 μg/mL of carbenicillin and incubated for 24 h at 37ºC. The presence of ZAP1 was confirmed, by PCR amplification using the primers listed in Table 2.2 (Fig. 7.2). After confirmation, the plasmid was extracted using ZR Plasmid Miniprep™-Classic Kit (Zymo Research), according to the manufacturer's instructions and sequenced (STABVida) to further confirm the presence and the integrity of the ZAP1 gene.

For the transformation of *C. glabrata* cells both WT and Δ*zap1* competent cells were made using the Frozen-EZ Yeast Transformation II Kit (Zymo research). Competent cells (50 μl) were transformed by adding 500 μL of frozen-EZ yeast solution 3 + 2 μL of either the empty plasmid or the plasmid with the gene of interest and incubating for 45 minutes at 30 ºC. After incubation cells were spread onto selective medium (SC -TRP) agar plates and incubated at 30 ºC for 48h. The colonies grown were streaked into a new plate with selective medium (SC -TRP).

2.3 Quantification of gene expression

Quantitative RT-PCR analyses were performed as previously described in (*76*). Biological triplicates of *C. glabrata* WT and Δ*zap1 strains* were grown until early exponential phase (OD$_{600}$ 0.8) in SC medium with or without zinc (SC +Zn and SC -Zn) and left untreated (Control) or treated with 32 µg/mL fluconazole for 1 h. 20 mL of cells were harvested by centrifugation at 3600*g* for 3 minutes. Total cellular RNA content was extracted using the phenol-chloroform method. Briefly, cells collected by centrifugation were resuspended in 1 mL of cold sterile bi-distillated water, transferred to a 2 mL Eppendorf, followed by centrifugation 1 minute maximum speed at 4ºC. The supernatant was discarded and 350 µL of LETS buffer (0.1 M LiCl; 0.01M Na$_2$EDTA; 0.01M Tris-HCl pH 7.4; 0.2% SDS, dissolved in bi-distillated sterile water) + 350 µL of phenol:chloroform (5:1) (lower phase) and glass beads were added to the pellet. Samples were vortexed for 10 minutes at 4ºC, placed on ice for 5 minutes and vortexed for another 10 minutes. Then, the samples were centrifuged at 14000*g* for 10 minutes, to separate the organic from the aqueous fraction, transferred it to a new Eppendorf and 1 mL of cold 100% ETOH was added to precipitate RNA overnight at -20 °C. RNA was collected by centrifuging for 30 minutes maximum speed at 4ºC. The supernatant was discarded and 1 mL of cold 70% ETOH was added (without resuspending) before centrifuging again at maximum speed for 15 minutes at 4 ºC. The supernatant was discarded, and the tubes left open until the pellets ere completely dry. After this step, 55 µL of RNAse free water was added and the tubes incubated at 65 ºC for 15 minutes to solubilize RNA. To confirm the integrity of RNA the samples were quantified (EPOCH) and its integrity was verified in a 1% agarose gel (Fig. 7.3). RNA samples were treated with DNAse (TURBO DNAse [Ambion®]) according to manufacturer's instructions, at 37ºC for 45 minutes. RNA integrity was again confirmed in an 1% agarose gel after treatment with DNase and the samples were quantified (EPOCH) (Fig. 7.4). RNA samples were purified using RNeasy® Mini Kit (QIAGEN) according to manufacturer's instructions. cDNA synthesis was performed using "Transcriptor Reverse Transcriptase" (ROCHE). Detection of the qRT-PCR products was done using the DNA intercalating compound SYBR Green (LightCycler LC-Faststart DNa MASTER SYBR Green I, (ROCHE)) and the qRT-PCR reaction was performed in a LightCycler® 480 equipment (ROCHE). Data was analyzed with the software LightCycler® Software 4.1. The *RPL10* gene (CAGL0K12826g, encoding the Ribosomal 60S subunit protein L10), was used as reference gene. All assays were performed using biological triplicates and technical duplicates. The primers used in qRT-PCR analyses are listed in Table 2.3.

Table 2.3: Primers used in qRT-PCR.

Primers	Sequence
CDR1_Fw	5' CATGGCCACTTTTGGTCTTT 3'
CDR1_Rv	5' CAGCAATGGAGACACGCTTA 3'
PDR1_Fw	5' CAGCAATGGAGACACGCTTA 3'
PDR1_Rv	5' AGTGGGCACGTCAGAGACAG 3'
ERG11_Fw	5' TATGGTCGCCTTGCCATT 3'
ERG11_Rv	5' GACCCATGGGATCCAGTAGA 3'
ERG3_Fw	5' GCTGTCTCTGCCATCCCTAC 3'
ERG3_Rv	5' TTCCTTAGACCGTGGTGCTC 3'
ERG5_Fw	5' GTAACATCGCTGGTCCTCGT 3'
ERG5_Rv	5' CGATGATGACGAACTTGTGG 3'
ZRT1_Fw	5' TGGTGGGTCATGTTCACAAC 3'
ZRT1_Rv	5' TTGAGTGATGTCCTGGTGGA 3'
ZRT2_Fw	5' CCATGGATTATGGCTTTTGC 3'
ZRT2_Rv	5' TCAATGCCTTTCGTGATCCT 3'
RPL10_Fw	5' GAGATTCTTTCCACTTGAGAGTCAGA 3'
RPL10_Rv	5' CTCTCATACCTTGTTGCAATCTATCC 3'

2.4 Cell membrane viability assays

C. glabrata WT and *Δzap1* mutant strains were grown until early exponential phase (OD_{600} 0.8) and left untreated (Control) or treated with 32 µg/mL fluconazole for 24 h. Cells were then harvested, washed 2 times with 1 mL of phosphate buffered saline (PBS), and resuspended in 1 mL of PBS containing 50 µg/mL of propidium iodide (PI) and incubated for 15 min in the dark. Samples were then washed 3 times with 1 mL of PBS and filtered with a 40 µm cell strainer. After filtered samples were proper diluted in 500 µL of PBS in cytometry tubes. Assays were performed in an S3e cell sorter (Bio-Rad) and PI signal was detected using the 488 nm excitation laser. Unstained cells were used to

establish the baseline of cells exhibiting positive PI signal. 100,000 cells were counted per sample, and five biological replicates were analyzed in each condition.

2.5 Ergosterol quantification

The quantification of ergosterol was performed by HPLC as described previously (*77*). *C. glabrata* WT and Δ*zap1* mutant strains were grown overnight in SC medium. Overnight cultures were diluted in 100 mL of fresh SC medium, OD_{600} 0.2, and grown until early exponential phase (OD_{600} 0.8). 80 mL of the culture were treated with 32 µg/mL fluconazole (Fluc) and 20 mL were left untreated (Control) for 24 h at 37ºC. After 24h the cells were transferred to tubes, centrifuged at max speed for 5 minutes and the pellets were resuspended in 2 mL of MiliQ water. 40 OD_{600} of each culture were transferred to new tubes, centrifuged at max speed for 2 minutes and resuspended in 1 mL of methanol and a volume of 100 µL of glass beads was added to the solution. This mixture was subjected to vortex agitation for 30 seconds and then incubated at 30 °C. After 1 h, samples were centrifuged at 4000 g for 7 min at 4 °C. The supernatant was recovered and centrifuged again at 9500 g for 10 min at 4 ºC. 10 µL of each sample were injected into a Symmetry C18 column (4.6 × 250 mm, 5 µm particle size, Waters Chromatography, USA), using a methanol/water (95:5% v/v) mixture as eluent. Column temperature was 30 °C and samples were kept at 10 °C. A standard curve prepared with ergosterol (Sigma Aldrich) diluted in methanol, was plotted to determine the amount of ergosterol present in each sample. All assays were performed using biological triplicates.

2.6 Fluconazole quantification

The quantification of fluconazole accumulation in *C. glabrata* WT and Δ*zap1* mutants was performed by HPLC as described previously (*77*). *C. glabrata* WT and Δ*zap1* mutant strain were grown overnight in SC medium. Cultures were used to inoculate 100 mL of fresh SC medium, OD_{600} 0.2, and grown until early exponential phase (OD_{600} 0.8). The protocol proceeded exactly as described for the quantification of ergosterol. 10 µL of each sample were injected into a Symmetry C18 column (4.6 × 250 mm, 5 µm particle size, Waters Chromatography, USA), using 80% ammonium acetate buffer with 15% acetonitrile and 5% methanol eluent mixture. Column temperature was 30 °C and samples were kept at 10 °C. A standard curve prepared with fluconazole (Sigma Aldrich) diluted in 80% ammonium acetate buffer with 15% acetonitrile and 5% methanol eluent mixture, was plotted to determine the amount of drug present in each sample. All assays were performed using biological triplicates.

2.7 Assessment of membrane potential

Measurements of membrane potential were performed according to (*78*), with few modifications. *C. glabrata* WT and Δ*zap1* mutant strain cells were grown overnight in SC medium. Cultures were used in the next day to inoculate 3 mL of SC medium at OD_{600} 0.2, and fresh cultures were left to grow until early exponential phase (OD_{600} 0.8). The culture was then split and left untreated or treated with 32 µg/mL of fluconazole for 24 h. Cells were harvested by centrifugation and washed with 1 mL of 0.1 mM $MgCl_2$, 2% (m/v) glucose in 10 mM MES pH 4. Pellets were resuspended in 1mL of 20 nM DioC6(3) in 2% glucose (10 mM MES, pH 4) and incubated at 37 °C, 180 rpm, in the dark for 2 h and then washed with 1 mL of 10 mM MES, pH 4 and filtered using a 40 µM cell strainer. Assays were performed in the S3e cell sorter (Bio-Rad) and DioC6(3) signal was detected using the 488 nm excitation laser and the FL1 detection channel. Unstained cells were used to establish the baseline of cells exhibiting positive DiOC6(3) signal. Five biological replicates of each condition were analyzed and a total of 100,000 cells were counted in each sample

2.8 Rhodamine 6G (R6G) assays

C. glabrata WT and Δ*zap1* mutant strains were grown overnight in SC medium. Overnight cultures were used to inoculate 3 mL of fresh SC medium at OD_{600} 0.2. Cultures were grown until early exponential phase (OD_{600} 0.8), harvested, washed twice with 1 mL of PBS, resuspended in 1 mL of PBS with 100 µM rhodamine 6g (R6G), and incubated for 30 min at 37 °C followed by 5 minutes on ice. Samples were then washed 3 times with 1 mL of PBS and filtered with a 40 µm cell strainer. Filtered samples were diluted in 500 µL of PBS in cytometry tubes. Assays were performed in an S3e cell sorter (Bio-Rad) and R6G signal was detected using the 488 nm excitation laser. Unstained cells were used to establish the baseline of cells exhibiting positive R6G signal. 100,000 cells were counted per sample, and five biological replicates were analyzed in each condition.

2.9 Quantification of phosphatidylinositol

The analysis of phosphatidylinositol levels was performed using the Phosphatidylinositol Assay Kit (Fluorometric) (Abcam, ab252900) with minor adaptations. Briefly, *C. glabrata* WT and Δ*zap1* strains were left untreated or treated with 32 µg/mL fluconazole for 24 h. 4 ODs of each culture were harvested by centrifugation. Cells were lysed using roughly 200 µL of glass beads in 200 µL of provided PI buffer and vortexed for 15 min at 4 °C. The cell homogenate was then recovered to conical 15 mL tubes, mixed with 750 µL of a 1:2 mixture of chlorofom:methanol (250 µL Chloroform: 500 µL Methanol) and vortexed thoroughly for 1 minute. 250 µL chloroform were added to the sample that was vortexed again for 30 seconds. Next, 250 µL ddH_2O were added to the tube, which after vortexing, was centrifuged at 1500 x g for 10 minutes at room temperature. Following this centrifugation step three distinct layers were visible: an upper phase containing methanol (aqueous

fraction), a thin layer of precipitated protein (at the interface), and the solubilized lipids in the lower organic phase. The upper phase was aspirated and discarded, taking care to avoid removing the lower phase. 500 µL of the "upper wash layer" (reagent provided by Phosphatidylinositol Assay Kit) were added to the lower phase, mixed vigorously, and spun down at 1500 x g for 10 minutes at room temperature. The upper phase was removed, and the process was repeated. Finally, the lower phase was collected and transferred to a new tube. The organic solvent was evaporated by placing the tubes in a dry heat block, within a fume hood, until no liquid was visible. Samples were re-suspended in 200 µL of PI Assay Buffer, vigorously vortexed and used immediately. PI Assay Buffer (30 µL) was added to 20 µL of the extracted lipids, in a 96 well plate, and incubated at 45°C for 2 hours. A volume of Reaction Mix reagent (50 µL) was then added to each well and the plate was incubated for 1 hour at 30 ºC. Fluorescence was recorded in a spectrofluorimeter - Varian Cary microplate reader-, endpoint mode and Ex/Em= 535/587 nm. This assay was performed using biological triplicates. A PI standard curve was made exactly as suggested by the manufacturer. The slope of the PI standard curve was calculated after subtraction of the control (without PI) from all standard fluorescent values. Values were plotted against the correspondent PI concentration and the slope was calculated and used to obtain the PI concentration in the samples.

2.10 Macrophage killing assays

The murine macrophage-like cell line J774A.1 was cultured in Dulbecco's modified Eagle's medium (DMEM, Biowest) supplemented with 10% fetal bovine serum (FBS) and sodium pyruvate (1 mM) at 37°C in 5% CO_2 atmosphere. For infection experiments J774A.1 cells were seeded in 24 - well plates, at a density of $3x10^5$ cells/well, cultured for approximately 18h and then washed with PBS before the infection with *C. glabrata* cells. *C. glabrata* cultures grown overnight in DMEM supplemented or not (control) with 32 µg/mL of fluconazole were harvested by centrifugation, washed twice with PBS and resuspended in DMEM. The OD600 of this suspension was measured to determine the volume required to obtain $6x10^4$ cells that were next added to each well, to obtain a multiplicity of infection (MOI) of 10:1 (macrophage:yeast). The number of cells in this inoculum was simultaneously confirmed by plating serial dilutions on YPD agar plates and counting CFUs after incubation at 37º C for 24 h (CFU at 0h). After 1h of infection at 37°C and 5% CO_2, the medium containing the non -phagocytosed cells was aspirated and wells were washed twice with PBS. The medium and washes were pooled and then serial diluted and plated on YPD agar plates for CFU counting (CFU non - phagocytosed cells). The number of phagocytosed cells (CFU at 1h) was calculated by subtracting the number of non - phagocytosed CFUs to the number of CFUs of the inoculum (CFU at 1h = CFU at 0h – CFU non - phagocytosed cells). Fresh DMEM was added to each well and plates were incubated at 37º C, 5% CO_2 for 24 h. After incubation, macrophages were lysed with sterile distilled water and the bottom of the wells was scrapped with a pipette tip and inspected under the microscope to guarantee the total recovery of the cells. Serial dilutions of this suspension were plated onto YPD agar plates and incubated for 24 h at 37º C, for CFU counting (CFU at 24h).

Yeast survival inside the macrophages was calculated according to the formula: %survival = [(CFU at 24h)/(CFU at 1h)] x 100.

2.11 Biofilm assays

To assess biofilm formation, *C. glabrata* WT and Δ*zap1* mutant cells were grown overnight in SC medium. The cultures were diluted to OD_{600} of 2 in 500 µL of SC medium and 100 µL of this cell suspension were transferred to the wells of a 96 well plate. 100 µL of a fluconazole solution diluted in SC medium were added to each well to a final concentration of 32 or 64 µg/mL. To the controls (cells without the drug), only 100 µL of SC medium were added to the wells. The plate was incubated for 24 hours at 37 ºC and 50 RPM. After incubation, all the medium was carefully removed from the wells and 100 µL of fresh SC medium plus 100 µL of the fluconazole solution or just 100 µL of SC medium (controls), were again added to each well following incubation for another 24 hours at 37 ºC, 50 RPM. After incubation, all medium was carefully removed, and the wells washed twice with 200 µL of PBS. After removing the PBS, the plate was left to dry for 15 minutes in a laminar airflow chamber. Next, 200 µL of 100 % ETOH were added to each well and the plate incubated at room temperature for 15 minutes. The ETOH was removed, and the plate left to dry for 10 minutes. 200 µL of 0.01% crystal violet were added to each well and the plate was incubated for 15 minutes. After another washing step with 200 µL of sterile water, wells were dried as described above and 200 µL of 100 % ETOH were added to each well and incubated for a period of 30 minutes, the well content was then resuspended and the OD_{595} was measured. Whenever needed, dilutions were made with 100 % ETOH. The assays were performed using biological quadruplicates.

To assess the impact of the mutant and drug in biofilms pre-formed, a similar protocol was followed, but the fluconazole solution (100 µL, with the concentration of 32 or 1250 µg/mL) diluted in SC medium was only added after the first 24 –hour incubation period.

3.1 Zap1 plays an important role in *Candida glabrata* survival under zinc deficiency conditions

We first tested whether, similarly to other yeasts, Zap1 is required for *C. glabrata* to grow under zinc-depleted conditions (*63-67*). For that, we compared the growth of the *CgΔzap1* mutant with that of the mutant transformed with a centromeric plasmid containing the gene (Δzap1<pZAP1>). Clearly, the deletion of *ZAP1* made *C. glabrata* cells more sensitive to zinc depletion (Fig. 3.1 A). The complementation of *CgΔzap1* mutant (Δzap1<pZAP1>) fully restored growth, whereas WT cells with extra copies of the gene (WT<pZAP1>) showed increased fitness (Fig. 3.1 A). In *Saccharomyces cerevisiae*, ScZap1 is a well-known regulator of high and low-affinity zinc transporters, encoded by the ScZRT1 and ScZRT2 genes, respectively (*63*). The genome of *C. glabrata* contains two ZRT-like sequences - CAGL0E01353g and CAGL0M04301g - that code for proteins with greater homology to ScZrt2 than to ScZrt1 (Fig. 3.1 B). Both genes are induced in zinc-limited cells (- Zn) in a Zap1-dependent manner, with the most pronounced effect observed for CAGL0E01353g (Fig. 3.1 C). Under zinc replete conditions (+ Zn), Zap1 appears to regulate CAGL0E01353g, but not CAGL0M04301g (Fig. 3.1 C). This latter regulation, however, does not affect yeast growth, since Δ*zap1*, Δ*CAGL0E01353g* and WT cells exhibited similar growth profiles under adequate zinc supply (Fig. 3.1 D).
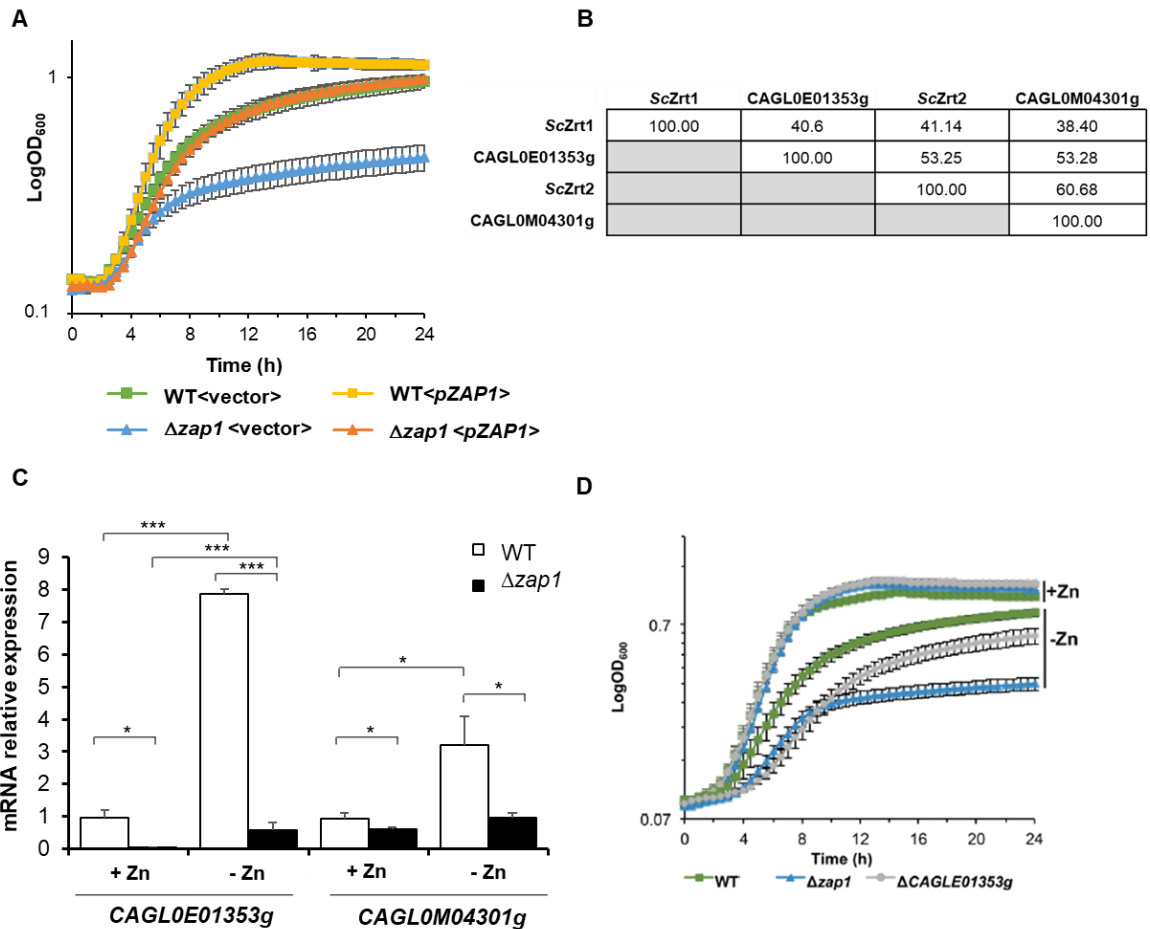
Figure 3.1: Zap1 is relevant for *Candida glabrata* to overcome zinc deficiency. A: Growth profile of *C. glabrata* WT and Δ*zap1* strains transformed with a plasmid containing the *ZAP1* gene (pZAP1) or the corresponding vector (vector), in zinc depleted medium. Growth was recorded for 24 h at 37ºC, by measuring OD_{600} at 30 min intervals. B: Percentage of amino acid identity between *Candida glabrata* ZRT-like genes (CAGL0E01353g and CAGL0M04301g) and *Saccharomyces cerevisiae* (Sc) *ZRT1* and *ZRT2*. C: The expression of CAGL0E01353g and CAGL0M04301g genes, in WT and Δzap1 cells, cultivated in SC medium with (+Zn, 0.4 mg/L $ZnSO_4$) or without zinc (-Zn), was measured by qRT-PCR. mRNA levels were normalized relatively to those of the reference gene RPL10. Significance of differences was calculated using student's T-test (* p-value < 0.05; *** p-value < 0.005). D: Growth profile of *C. glabrata* WT, ΔCAGL0E01353g and Δ*zap1* strains in zinc-depleted (-Zn) or replete (+Zn) medium. Growth was recorded as described above.

3.2 Zap1 is a negative regulator of biofilm formation

C. albicans Zap1 was shown to be a negative regulator of a major biofilm matrix component (*65*), which led us to investigate whether Zap1 in *C. glabrata* could also have a regulatory role in biofilm formation. The results (Fig. 3.2 A) show that in the absence of Zap1 there is an increase in biofilm formation. The presence of fluconazole also contributes to the increase in biofilm formation both in WT and mutant strains (Fig. 3.2 A). We also tested if fluconazole could affect preformed biofilms. We found that an effect similar to the one described above was only evident for the highest concentration of the fluconazole tested, for WT cells. Taken together, these results show that fluconazole is an ineffective drug against *C. glabrata* biofilms and may actually promote their formation (Fig. 3.2 B). Moreover, Zap1 appears to be a negative regulator of biofilm formation.
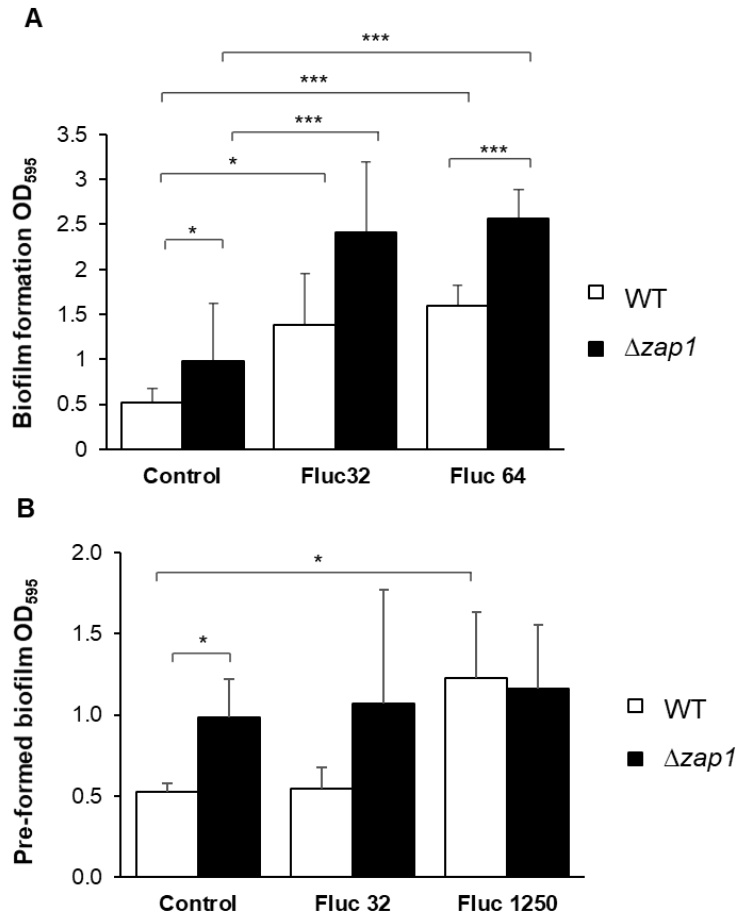
Figure 3.2: Zap1 deletion, as well as fluconazole treatment increase biofilm formation. A: Biofilm formation of WT and Δ*zap1* treated and untreated with fluconazole (Fluc 32, 64 are 32, 64 µg/mL fluconazole). B: Impact of fluconazole in pre-formed biofilm (Fluc 32, 1250- are 32, 1250 µg/mL fluconazole). Significance of differences was calculated using student's T-test (*** p-value < 0.005; *p-value < 0.05).

3.3 Deletion of *ZAP1* gene increases the sensitivity of several yeasts to fluconazole, possibly by affecting cell permeability

According to recent results obtained in our laboratory, deletion of *ZAP1* in *C. glabrata*, renders the mutant *CgΔzap1* more sensitive to fluconazole than the WT strain (Gaspar-Cordeiro *et al.*, under review). Since fluconazole affects the ergosterol composition of the membrane, which may alter membrane fluidity, we analyzed cell membrane permeability by flow cytometry using propidium iodide (PI), a fluorescent intercalating agent that binds DNA. *CgΔzap1* cells showed a 30% increase in fluorescence when compared to the wild-type (WT) strain, after fluconazole treatment (Fig. 3.3 A). To ensure that this difference was due to altered permeability and not increased cellular death in the mutant (as PI is excluded from viable cells but enters death cells), we compared the survival rates of both WT and mutant strains, by counting CFUs. The results showed no significant difference between the number of CFU/mL in WT and mutant cultures, regardless of the condition (Fig. 3.3 B). As such, the differences between WT and mutant observed in Fig. 3.3 B upon fluconazole treatment are probably due to differences in plasma membrane permeability. Thus, we conclude that fluconazole

treatment has a more pronounced effect on the permeability of *CgΔzap1* mutant cells than on that of the WT cells.

Remarkably, the effect of *ZAP1* deletion on fluconazole susceptibility does not appear to be exclusive to *C. glabrata*, as both *Candida albicans* and *Saccharomyces cerevisiae* mutant strains display a similar phenotype (Fig. 3.3 C). These data show that the involvement of Zap1 in fluconazole resistance is not species specific.
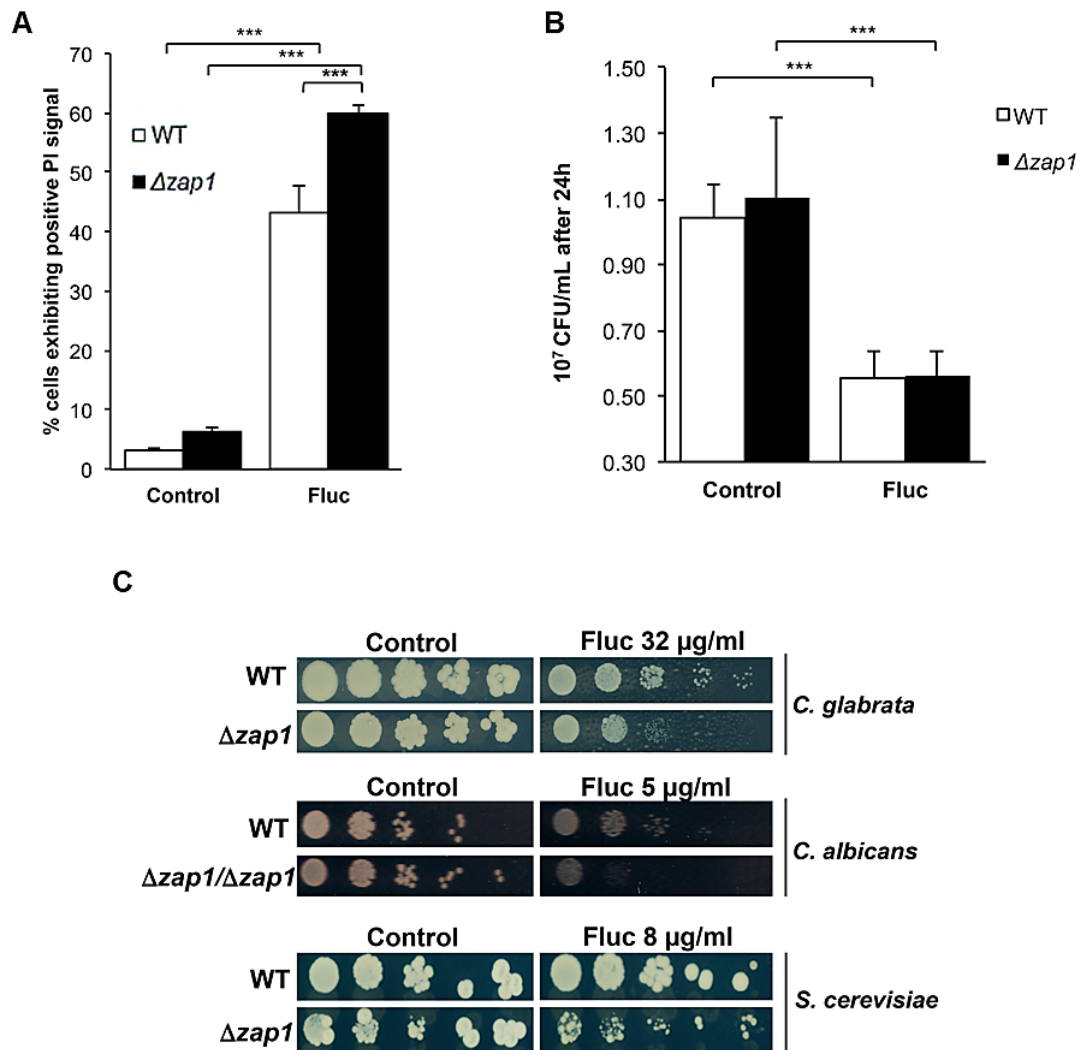
Figure 3.3: Deletion of *ZAP1* increases fluconazole sensitivity in yeasts. A: Accumulation of propidium iodide (PI) in *C. glabrata* WT and *Δzap1* cells left untreated (Control) or treated with 32 µg/mL fluconazole (Fluc) for 24 h was measured by flow cytometry. B: Cell viability of the 24 h cultures was evaluated by diluting cells in sterile PBS to a final concentration of 103 cells/mL. A sample (100 µL) of the suspension was inoculated on solid YPD medium and incubated at 37 °C. CFUs were counted after 24 h. Significance of differences was calculated using student's T-test (*** *p*-value < 0.005). C: Growth sensitivity of *C. glabrata* (WT), *C. albicans* (DAY185) and *S. cerevisiae* WT (BY4742) and the respective *Δzap1* mutant strains in SC agar plates (Control) containing the indicated concentrations of fluconazole (Fluc). Growth was recorded after 48 h at 37 ºC (*C. glabrata*), 30 ºC (*C. albicans*), or 72 h at 30 ºC (*S. cerevisiae*).

3.4 The ergosterol depletion caused by fluconazole is more pronounced in the *CgΔzap1* than in wild type cells

The fact that fluconazole is an inhibitor of the Erg11 enzyme, together with previous reports suggesting a role of Zap1 in the regulation of the *ERG* genes (*65, 72*) and the increased permeability of mutant cells (Fig. 3.2 A), led us to investigate whether the ergosterol biosynthesis could be affected by the absence of Zap1. Although the levels of ergosterol did not differ between WT and *CgΔzap1* under control conditions, after fluconazole treatment, a more pronounced depletion of ergosterol was observed in the mutant (Fig. 3.4 A). In order to clarify whether this observation could be a consequence of the potential regulation of *ERG* genes by Zap1, we evaluated the expression of *ERG3*, *ERG5* and *ERG11*, which encode key enzymes of ergosterol biosynthesis (*79*). The results showed that the expression of *ERG11* did not change in cells depleted of Zap1, but both *ERG3* and *ERG5* were upregulated in the *CgΔzap1* mutant after treatment with fluconazole, suggesting that, in this particular condition, Zap1 negatively affects the expression of these genes (Fig. 3.4 B).
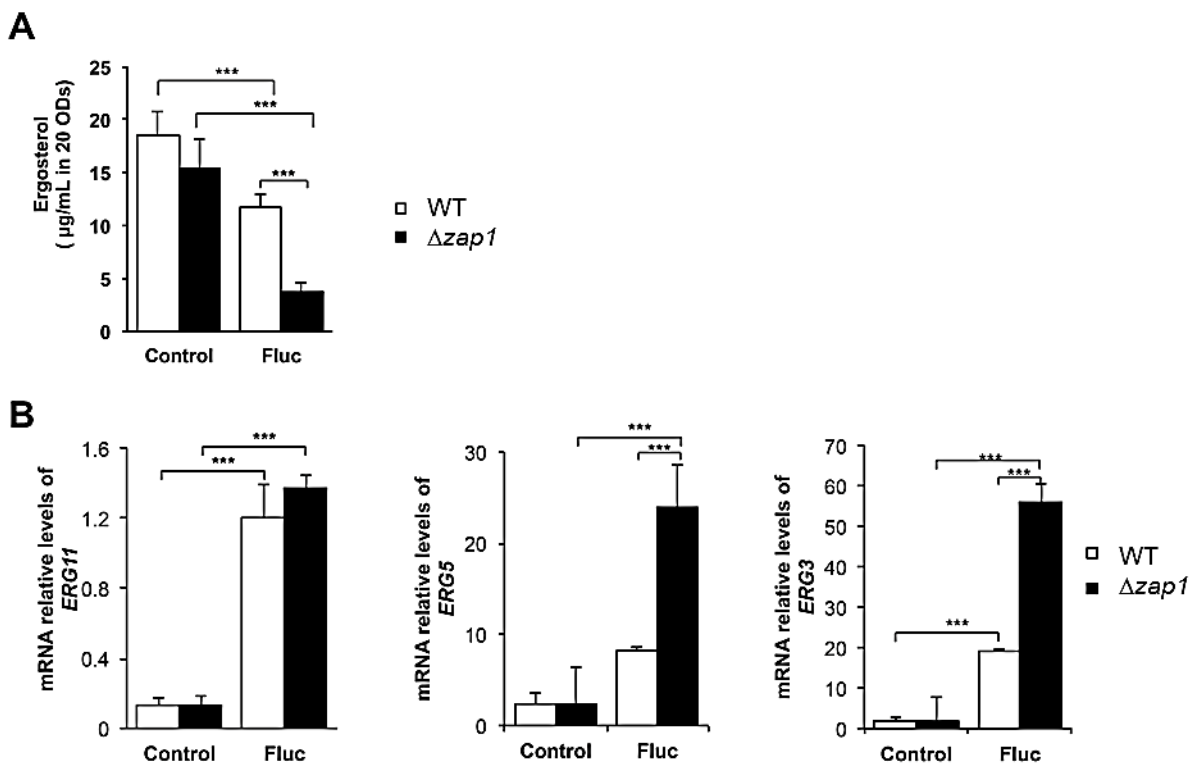
Figure 3.4: The ergosterol metabolism is affected in *CgΔzap1* cells treated with fluconazole. A: The ergosterol content of *C. glabrata* WT and Δ*zap1* cells left untreated (Control) or treated with 32 µg/mL fluconazole (Fluc), for 24 h, was measured by HPLC. B: The expression of the ERG11, ERG5 and ERG3 genes was evaluated by qRT-PCR in *C. glabrata* WT and Δzap1 cells untreated (Control) or treated with 32 µg/mL fluconazole (Fluc), for 1 h. Significance of differences was calculated using student's T-test (*** *p*-value < 0.005; ***p*-value < 0.05).

3.5 The repression of *PDR1* and *CDR1* by Zap1 contrasts with the higher accumulation of fluconazole in the *CgΔzap1* mutant

In line with the previous observation, we found that *CgΔzap1* cells accumulate twice as much fluconazole as the WT strain (Fig. 3.5 A). Using flow cytometry, we analyzed the drug efflux using the fluorescent dye rhodamine 6G, which is a known substrate of drug efflux pumps such as Cdr1 (*80*). The accumulation of rhodamine 6G prompted us to conclude that drug efflux is impaired in the *CgΔzap1* mutant (Fig. 3.5 B). Our first hypothesis, was that this impairment could be due to the involvement of Zap1 in the regulation of the multidrug efflux pump gene *CDR1*, as indicated by several transcriptomic studies (*65, 72, 81, 82*). Surprisingly, *CDR1* expression was strongly upregulated in the *CgΔzap1* mutant when exposed to fluconazole (Fig. 3.5 C), suggesting that Zap1 is a negative regulator of *CDR1* in the presence of the drug. Since Pdr1 is the main regulator of the *CDR1* gene (*58, 83*), we wondered if Zap1 could be controlling the expression of *PDR1* and, therefore, indirectly regulating *CDR1* expression. The results indicated that, in control conditions, *ZAP1* deletion strongly induces *PDR1*, suggesting that Zap1 is indeed a negative regulator of the gene (Fig. 3.5 D). Interestingly, the induction of *PDR1* observed in WT cells after treatment with fluconazole was no longer observed in the *CgΔzap1* mutant, as *PDR1* levels remained similar to those of untreated cells (Fig. 3.5 D).
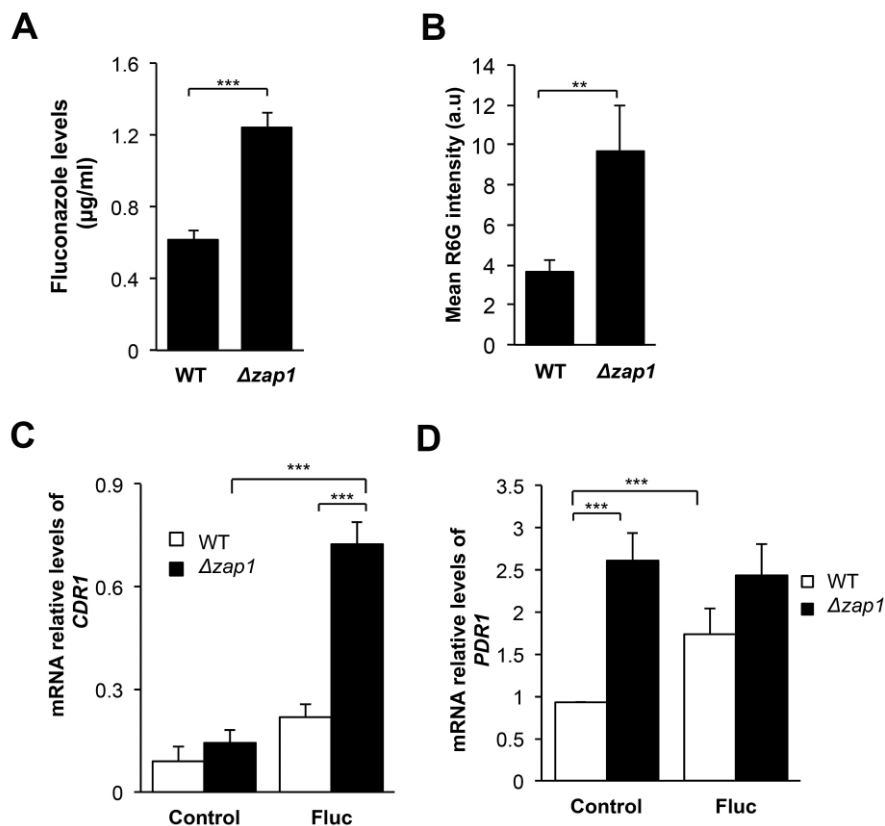
Figure 3.5: Zap1 is a negative regulator of *CDR1* and *PDR1*. A: The accumulation of fluconazole in WT and Δ*zap1 C. glabrata* cells treated with 32 µg/mL fluconazole (Fluc) for 24 h was measured by HPLC. B: Rhodamine 6G accumulation in *C. glabrata* WT and Δ*zap1* cells exposed to 32 µg/mL fluconazole (Fluc) for 24 h, was

performed by flow cytometry. Values are the mean of five independent biological replicates with 100,000 cells counted per condition. The expression of the C: *CDR1* gene and D: *PDR1* was determined by qRT-PCR in *C. glabrata* WT and Δ*zap1* cells untreated (Control) or treated with 32 µg/mL fluconazole (Fluc), for 1 h. Significance of differences was calculated using student's T-test (*** p-value < 0.005; **p-value < 0.01).

3.6 Plasma membrane potential and composition are altered in the *CgΔzap1* mutant

The fact that *CgΔzap1* cells are unable to effectively detoxify fluconazole, despite the marked upregulation of *CDR1* (Fig. 3.5), made us question whether the activity of drug exporters could be affected. In *Saccharomyces cerevisiae*, Zap1 is involved in the regulation of phospholipid biosynthesis (*73, 75*). As phospholipids are the main component of plasma membranes, we hypothesized that the lack of Zap1 could affect membrane phospholipid composition. To test this possibility, we analyzed phosphatidylinositol levels, which is a phospholipid whose biosynthesis in *Saccharomyces cerevisiae* is dependent on Zap1 (*74*). In line with a possible role of *ZAP1* in phosphatidylinositol biosynthesis, we found that under control conditions, the levels of phosphatidylinositol were significantly reduced in the mutant (Fig. 3.6 A). After treatment with fluconazole the phosphatidylinositol content of mutant and WT strains decreased, with the levels in the former being consistently lower (Fig. 3.6 A). Moreover, the *CgΔzap1* mutant exhibited a noticeable membrane hyperpolarization compared to the WT strain (Fig. 3.6 B). As reported by other authors (*84*), we found that fluconazole triggered membrane hyperpolarization, but the effect continued to be more evident in the *CgΔzap1* mutant (Fig. 3.6 B). These results suggest that, in the mutant, the marked changes in the membrane composition (phosphatidylinositol and ergosterol) could affect the physicochemical properties of the membrane, which, in turn, might compromise membrane-associated processes, such as fluconazole efflux.
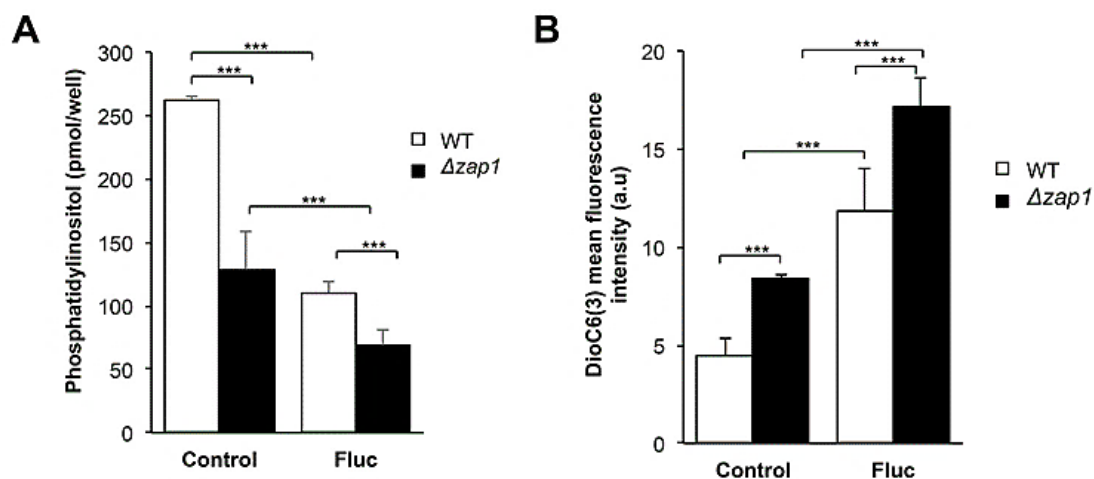
Figure 3.6: Plasma membrane composition and potential are affected by *ZAP1* deletion. A: The phosphatidylinositol content of *C. glabrata* WT and Δ*zap1* mutant cells left untreated (Control) or treated with 32 µg/mL fluconazole (Fluc) for 24 h was determined using a fluorimetric-based assay. B: DiOC6(3) fluorescence signal detection in *C. glabrata* WT and Δ*zap1* cells, left untreated (Control) or treated with 32 µg/mL fluconazole (Fluc), was performed by flow cytometry. Values are the mean of five independent biological replicates with 100,000 cells counted per each condition. Significance of differences was calculated using student's T-test (*** p-value < 0.005).

3.7 Deletion of Zap1 does not impact the cell size

A study by Dhara Malavia and colleagues (*85*) showed that in response to zinc limitation *Candida albicans*, *C. dubliniensis* and *C. tropicalis*, have alterations in their morphology resulting in enlarged spherical cells (*85*). As *CgΔzap1* mutant cells are zinc-depleted compared to WT cells (our group's data), to rule out the possibility that a similar effect was occurring in the mutant, which would impact the experiments done so far, we observed under the microscope WT and mutant cells untreated and treated with fluconazole. The results indicate that there are no differences in size of WT and *CgΔzap1* grown on SC medium left untreated or treated with fluconazole for 24h (Fig. 3.7).
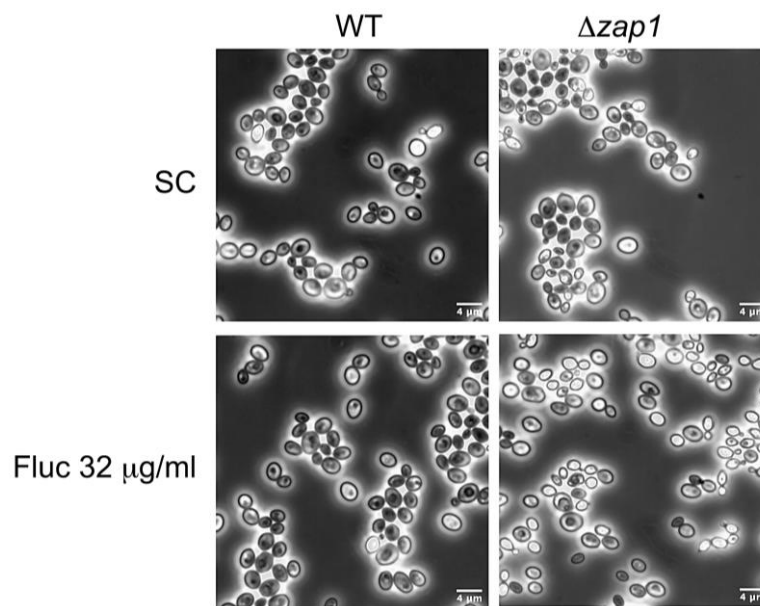
Figure 3.7: *CgΔzap1* and WT cells have similar sizes. *C. glabrata* WT and Δ*zap1* mutant strains untreated (Control) or treated with 32 µg/mL fluconazole (Fluc) for 24h observed under the microscope. Pictures were taken using a phase contrast objective Uplan F1 100× and captured with a CCD camera Andor IxonEM (Andor Technologies) using Metamorph version 5.8 (Universal Imaging).

3.8 Fluconazole concurs with macrophages for *C. glabrata* killing

In order to evaluate if macrophages synergize with fluconazole to kill *C. glabrata*, we first established the optimal conditions to perform the experiment. First, we observed that growing *C. glabrata* pre-inoculum in SC medium and then change the medium to DMEM caused the cells to have abnormal growth. This led us to grow the cells from the beginning in DMEM instead of SC medium. Next, we tested different MOI (Multiplicity of infection), 100:1, 10:1 and 5:1, to see if there were some differences. Since no significant differences were obtained using different MOIs (data not shown), we decide to proceed with the 10:1 MOI. We also tested if adding interferon gamma (IFN-γ), which is a stimulator of macrophages, would impact the results. For that, prior to the infection we washed the macrophages with 1 mL of PBS and added 500 µL of 5 ng/mL IFN- γ solubilized in DMEM, followed by an incubation for 3 hours at 37ºC with 5% CO_2. Then, the infection was performed as described for the

final experiment (section 2.10). No significant differences were observed, regardless of the strains and treatments used, and therefore IFN-γ was omitted from the following experiments. Moreover, the treatment with fluconazole was initially performed at the same time that yeast cells were added to the monolayer of macrophages, but no differences were seen among all tested conditions and strains that led us to hypothesize that fluconazole did not have time to act on *C. glabrata* cells before phagocytosis occurred. Therefore, we decided to perform fluconazole treatment on *C. glabrata* cells prior macrophage infection.

Once established the ideal conditions for macrophage infection assays, we investigated if targeting Zap1 could be an interesting strategy to improve the efficacy of fluconazole in the context of infection. For that, we evaluated whether macrophages synergized with fluconazole for antifungal activity against *C. glabrata* and also analyzed the impact of *ZAP1* deletion in this process.

Unexpectedly we observed that under control conditions, deletion of *ZAP1* improved the ability of *C. glabrata* to survive macrophage killing (Fig. 3.8 A). Upon fluconazole exposure, both strains became equally susceptible to macrophage killing, indicating a combined effect between macrophages and the drug. This effect was more evident in the *CgΔzap1* mutant (35% of growth reduction) than in WT cells (16% of growth reduction), which further reinforces the importance of Zap1 in the adaptation to fluconazole. Of note, none of the conditions tested interfered with phagocytosis (Fig. 3.8 B). As a first approach to understand why *CgΔzap1* would have increased fitness inside the macrophage, we tested stress conditions that macrophages use to kill cells, namely low pH, oxidative and nitrosative stresses. In all of the tested conditions *CgΔzap1* showed no difference or was even more sensitive than WT cells (Fig. 3.9). A recent study by Riedelberger M. *et al.* (*34*) showed that macrophages use zinc intoxication and ROS production to eliminate engulfed *C. glabrata* cells. This led us to test if the increased survival of *CgΔzap1* in macrophages could be due to an impairment of zinc homeostatic mechanisms, which, in this particular case, could be beneficial due to the attenuation of macrophage-driven zinc intoxication. Since in the mutant zinc transporters are down regulated (Fig. 3.1 C), we assume that zinc intoxication would not be as effective as in the WT strain. Corroborating this notion, the results showed that *CgΔzap1* strain is more resistant than the WT to a combination of zinc excess and oxidative stress (Fig. 3.9).
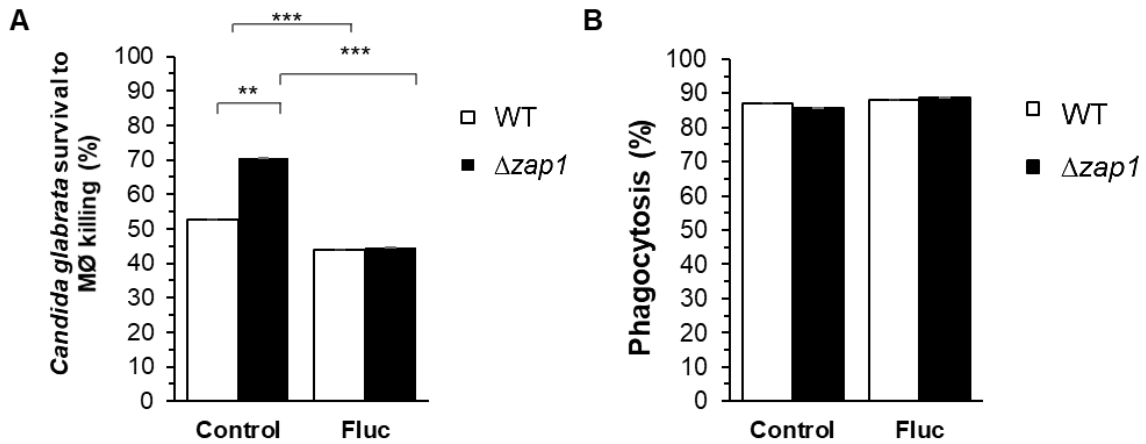
Figure 3.8: Deletion of *ZAP1* makes *C. glabrata* cells less susceptible to macrophage killing. A: The survival of *C. glabrata* WT and Δ*zap1* mutant strain untreated (Control) or treated with 32 μg/mL fluconazole (Fluc) and exposed to murine J774.1A macrophages (MØ), was determined by plating the appropriate cell dilutions of internalized yeasts 24 h post-infection in YPD agar plates and counting the colony forming units (CFUs). Significance of differences was calculated using student's T-test (*** p-value < 0.005; ** p-value < 0.05). B: The non-phagocyted *C. glabrata* cells WT and Δ*zap1* mutant strain untreated (Control) or treated with 32 μg/mL fluconazole (Fluc) and exposed to murine J774.1A macrophages (MØ), was determined by plating the appropriate cell dilutions of non-phagocyted cells after 1h contacting with macrophages in YPD agar plates and counting the colony forming units (CFUs).
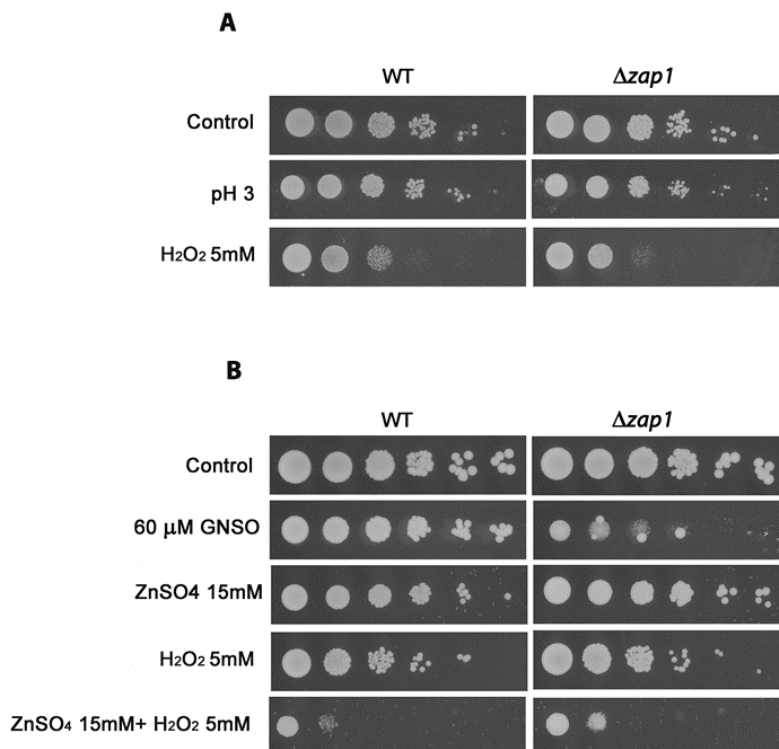
Figure 3.9: *CgΔzap1* is more sensitive to oxidative and nitrosative stress, but more resistant to the combination of H_2O_2 and zinc. Growth of *C. glabrata* (WT) and Δ*zap1* mutant strain in SC agar plates (Control) under the indicated conditions. Growth was recorded after incubation for A: 24 h or B: 48 h at 37°C.

34

Chapter 4 – Discussion

Azoles and in particular, fluconazole, are widely used antifungals due to their safety profile and low cost. *C. glabrata* invasive infections, although not as frequent as those caused by *Candida albicans,* are associated with higher rates of mortality and morbidity. Possibly contributing to this scenario is the inherent tolerance of *C. glabrata* to fluconazole, the most prescribed antifungal agent in the world (*15, 16*). Therefore, understanding how this yeast deals with fluconazole has been the focus of extensive research.

In this work, we show that the transcription factor Zap1 plays a role in the response of *C. glabrata* to fluconazole. We first confirmed the role of Zap1 in *C. glabrata* under zinc deficiency conditions. As in other yeast species (*63, 65-67*), Zap1 controls the response to zinc depletion, possibly through the regulation of ZRT-like genes (Fig. 3.1)

We found that Zap1 regulates *C. glabrata* biofilm formation. Biofilms function as physical barriers that prevent entry and activity of drugs and other toxic compounds. Deletion of Zap1 led to an increase in biofilm formation, similarly to what happens in *C. albicans* (*65*), suggesting that in *C. glabrata* Zap1 is also a repressor of biofilm formation. Pdr1 is known to positively regulate the expression of genes encoding cell wall adhesins, which are important for the first steps of biofilm formation (*86*). In the *CgΔzap1* mutant, *PDR1* is highly upregulated (Fig. 3.5 D), therefore it is conceivable that the hypothetical increase in adhesins expression can positively impact biofilm formation (Fig. 3.2 A) (*87*).

ZAP1 deletion increases the sensitivity to fluconazole not only in *C. glabrata*, but also in other yeast species, namely, *C. albicans* and *S. cerevisiae* (Fig. 3.3). As mentioned before, fluconazole inhibits the enzyme encoded by *ERG11* gene, which is a key enzyme in the ergosterol biosynthesis pathway. The results showed that in *CgΔzap1* mutant*,* ergosterol levels are reduced (Fig. 3.4), which is in agreement with its greater accumulation of fluconazole compared to the WT strain (Fig. 3.5). Remarkably, while *ZAP1* deletion did not affect the expression of *ERG11*, it significantly increased the expression of *ERG3* and *ERG5* after treatment with fluconazole (Fig. 3.4), possibly to counteract the depletion of ergosterol levels. Zap1 is a negative regulator of *ERG* genes in *C. albicans*, but a positive regulator of these genes in *S. cerevisiae* (*65, 72, 81, 82*). Despite the phylogenetic proximity between *C. glabrata* and the model yeast *Saccharomyces cerevisiae* (*88*) (Fig. 4.1), this work suggests that *ZAP1* acts as a negative regulator of some *ERG* genes, resembling *C. albicans* in this regard.
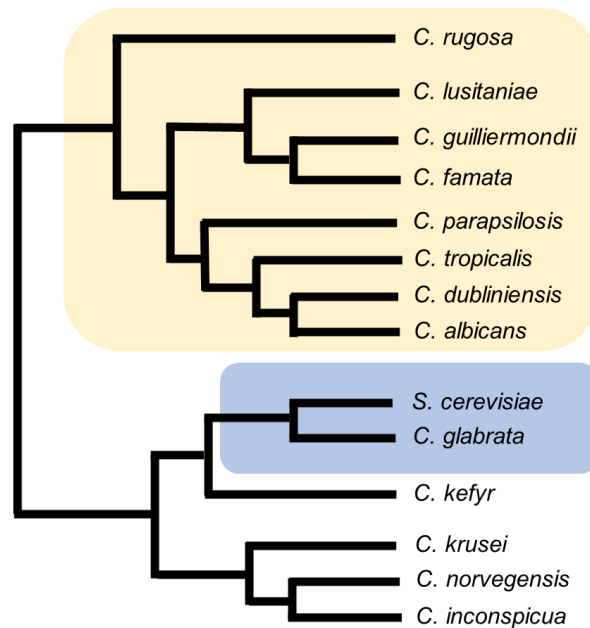
Figure 4.1: Schematic representation of the phylogeny of *Candida albicans* and non-*albicans* species. (Adapted from N. Papon, V. Courdavault, M. Clastre, R. J. Bennett, Emerging and emerged pathogenic Candida species: beyond the Candida albicans paradigm. *PLoS Pathog* **9**, e1003550 (2013)).

Fluconazole accumulation in the *CgΔzap1* mutant may result from deficient drug efflux or, alternatively, from an increase in drug uptake, which in other pathogenic fungi enters the cells by facilitated diffusion (*89*). Several reports indicate that Zap1 regulates important drug efflux transporters both in *S. cerevisiae* and *C. albicans* (*65, 72, 81, 82*). Thus, we put forward the hypothesis that the accumulation of fluconazole observed in the mutant *CgΔzap1* could be due to the downregulation of drug efflux genes, such as *CDR1*. However, contrary to our expectations, *CDR1* expression was highly upregulated in the mutant, as well as the expression of the gene encoding its main regulator, *PDR1* (*58, 83, 90*) (Fig. 3.5). Under control conditions, deletion of *ZAP1* did not interfere with the *CDR1* expression, but remarkably upregulated *PDR1*. Even though transcriptional regulation is an important feature of Pdr1 activity (*90*) direct azole binding is fundamental for its full activity. (*91*) Therefore, if Zap1 downregulates *CDR1* expression via the repression of *PDR1*, the lack of *CDR1* upregulation in untreated *CgΔzap1* cells, despite the maximum expression of *PDR1*, may be due to the deficient activation of Pdr1 in the absence of fluconazole. Moreover, *PDR1* expression showed no difference between control conditions and treatment with fluconazole in the mutant, which indicates that in the absence of Zap1 the expression of *PDR1* reaches its maximum level even without fluconazole addition. But the question remains: why does fluconazole accumulate in mutant cells if *PDR1* and *CDR1* are overexpressed? One possible explanation is that Cdr1 function is impaired in *CgΔzap1*, as suggested by the mutant inability to expel rhodamine 6G (Fig. 3.5).

In *S. cerevisiae*, Zap1 affects phospholipid synthesis, through the regulation of phosphatidylinositol synthase gene, *PIS1*, and phosphatidate phosphatase, *PAH1* (*73, 74, 92*). Phospholipids are important components of the cellular membrane and are essential for the correct function of membrane proteins; it is possible that the deregulation of phospholipid biosynthesis in

CgΔzap1 cells, together with ergosterol depletion, (Fig. 3.4) leads to extensive disruption of the membrane function. Accordingly, we observed that *CgΔzap1* cells have a lower phosphatidylinositol content (Fig. 3.6). Several studies showed that phosphatidylinositides are important for yeasts to tackle azole stress (*93, 94*). In particular, the trafficking and activity of the efflux pump Cdr1 in the plasma membrane is dependent on phosphatidylinositol-4-phosphate (*95*). Moreover, Elicharova and Sychrova showed that fluconazole-driven membrane hyperpolarization, is an important part of fluconazole toxicity, as it affects the regular membrane permeability (*84*). It has been shown that the hyperpolarization, as well as a defective sterol composition of the plasma membrane, affects the function and localization of the multidrug efflux pump Cdr1 (*96*). Cells with low levels of ergosterol, have lower membrane potential and Cdr1 is mislocalized in the vacuoles (*97*). Thus, we hypothesize that the changes in plasma membrane properties observed in *CgΔzap1* may affect the activity of Cdr1, which could explain the accumulation of fluconazole, despite the overexpression of the gene. In the future it would be interesting to assess the localization of Cdr1 in the mutant *CgΔzap1* after treatment with fluconazole.

Interestingly, deletion of *ZAP1* gave *C. glabrata* a competitive advantage to resist macrophage killing. Since Zap1 regulates a wide range of genes (*65, 72*), a possible explanation is that *CgΔzap1* mutant cells could have gained advantage to survive the macrophage hostile environment. However, *CgΔzap1* is as resistant or even more sensitive than the WT to any of the phagolysosome stresses (*98*) such as low pH, oxidative and nitrosative stress (Fig. 3.9). A recent study revealed that to kill engulfed *C. glabrata* cells, macrophages use zinc bursts combined with the production of ROS (*34*). Interestingly we found that *CgΔzap1* is less susceptible to this combination than WT cells (Fig. 3.9 B). Therefore, it seems very likely that disruption of zinc homeostasis in the mutant makes cells more resistant to the combination of zinc excess and ROS that would benefit yeast survival within the phagolysosome. Similarly, infection of murine macrophages with *Cryptococcus gattii* Δ*zap1* mutant cells has been shown to result in higher CFU counts as compared to the WT (*67*). Nevertheless, *in vivo* models of infection of the Δ*zap1* mutant of, *Cryptococcus gattii* (*67*), *Candida dublinensis* (*66*), *Candida albicans* (*82*) and *Aspergillus fumigatus* homolog mutant (Δ*zafA*) (*99*), showed attenuated virulence. Therefore, we cannot exclude the possibility that *CgΔzap1* could also be less virulent than WT in *in vivo* models of infection, and concomitantly make the yeast more sensitive to fluconazole treatment. That being the case, targeting Zap1 could be considered a promising strategy to enhance the effectiveness of fluconazole.

Chapter 5 – Conclusion

The work developed in the context of this thesis aimed to unveil the role of the transcription factor Zap1 in the response of *C. glabrata* to fluconazole and to confirm its role in zinc homeostasis.

Our results clearly show that Zap1 regulates *C. glabrata* adaptation to zinc depletion, possibly by regulating zinc uptake. Zap1 also acts as a negative regulator of biofilm formation as well as a negative regulator of the drug efflux gene *CDR1* via the repression of the transcription factor *PDR1*. Despite the overexpression of *CDR1*, mutant cells accumulate more fluconazole and have lower ergosterol levels. We propose that this apparent paradox is due to the fact that depletion of Zap1 also induces profound alterations in the plasma membrane that, together with ergosterol depletion, prevents the proper functioning of Cdr1.

We propose that following fluconazole exposure, *C. glabrata* downregulates the expression of *ZAP1* (Gaspar-Cordeiro *et al*, under review) to fine tune the expression of *PDR1* and *CDR1* genes and therefore maximize drug efflux. However, the complete abrogation of *ZAP1* prompts a different scenario, where, despite the upregulation of *CDR1* and *PDR1*, alterations of the plasma membrane negatively impact the function of Cdr1 and, consequently, reduce drug extrusion.

Chapter 6 – Bibliography

1.   P. R. Murray, K. S. Rosenthal, M. A. Pfaller, *Medical microbiology*. (Elsevier, Philadelphia, 2021).

2.   S. Vallabhaneni, R. K. Mody, T. Walker, T. Chiller, The Global Burden of Fungal Diseases. *Infect Dis Clin North Am* 30, 1-11 (2016).

3.   G. Janbon, J. Quintin, F. Lanternier, C. d'Enfert, Studying fungal pathogens of humans and fungal infections: fungal diversity and diversity of approaches. *Genes Immun* 20, 403-414 (2019).

4.   F. Bongomin, S. Gago, R. O. Oladele, D. W. C. P. Denning, Global and Multi-National Prevalence of Fungal Diseases-Estimate Precision. *J Fungi (Basel)* 3, (2017).

5.   P. Vandeputte, S. Ferrari, A. T. Coste, Antifungal resistance and new strategies to control fungal infections. *Int J Microbiol* 2012, 713687 (2012).

6.   D. A. Enoch, H. A. Ludlam, N. M. Brown, Invasive fungal infections: a review of epidemiology and management options. *J Med Microbiol* 55, 809-818 (2006).

7.   S. Brunke, B. Hube, Two unlike cousins: *Candida albicans* and *C. glabrata* infection strategies. *Cell Microbiol* 15, 701-708 (2013).

8.   J. Perlroth, B. Choi, B. Spellberg, Nosocomial fungal infections: epidemiology, diagnosis, and treatment. *Med Mycol* 45, 321-346 (2007).

9.   S. B. Wey, M. Mori, M. A. Pfaller, R. F. Woolson, R. P. Wenzel, Risk factors for hospital-acquired candidemia. A matched case-control study. *Arch Intern Med* 149, 2349-2353 (1989).

10.   S. Silva, M. Negri, M. Henriques, R. Oliveira, D. W. Williams, J. Azeredo, *Candida glabrata*, *Candida parapsilosis* and *Candida tropicalis*: biology, epidemiology, pathogenicity and antifungal resistance. *FEMS Microbiol Rev* 36, 288-305 (2012).

11.   L. Ostrosky-Zeichner, J. H. Rex, J. Bennett, B. J. Kullberg, Deeply invasive candidiasis. *Infect Dis Clin North Am* 16, 821-835 (2002).

12.   P. G. Pappas, M. S. Lionakis, M. C. Arendrup, L. Ostrosky-Zeichner, B. J. Kullberg, Invasive candidiasis. *Nat Rev Dis Primers* 4, 18026 (2018).

13.   M. A. Pfaller, D. J. C. P. Diekema, Epidemiology of invasive candidiasis: a persistent public health problem. *Clin Microbiol Rev* 20, 133-163 (2007).

14.   J. A. Paiva, J. M. Pereira, A. Tabah, A. Mikstacki, F. B. Carvalho, D. Koulenti, S. Ruckly, N. Çakar, B. Misset, G. Dimopoulos, M. Antonelli, J. Rello, X. Ma, B. Tamowicz, J. Timsit, Characteristics and risk factors for 28-day mortality of hospital acquired fungemias in ICUs: data from the EUROBACT study. *Crit Care* 20, 53 (2016).

15.   M. A. Pfaller, D. R. Andes, D. J, Diekema, D. L. Horn, A. C. Reboli, C. Rotstein, B. Franks, N. E. Azie, Epidemiology and outcomes of invasive candidiasis due to non-albicans species of Candida in 2,496 patients: data from the Prospective Antifungal Therapy (PATH) registry 2004-2008. *PLoS One* 9, e101510 (2014).

16.   M. A. Pfaller, D. J. Diekema, J. D. Turnidge, M. Castanheira, R. N. C. P. Jones, Twenty Years of the SENTRY Antifungal Surveillance Program: Results for *Candida* species from 1997-2016. *Open Forum Infect Dis* 6, S79-S94 (2019).

17.   J. M. Gancedo, Control of pseudohyphae formation in *Saccharomyces cerevisiae*. *FEMS Microbiol Rev* 25, 107-123 (2001).

18.   T. Gabaldón *et al.*, Comparative genomics of emerging pathogens in the *Candida glabrata* clade. *BMC Genomics* 14, 623 (2013).

19. P. L. Fidel, J. A. Vazquez, J. D. C. P. Sobel, *Candida glabrata*: review of epidemiology, pathogenesis, and clinical disease with comparison to C. albicans. *Clin Microbiol Rev* 12, 80-96 (1999).

20. C. F. Rodrigues, S. Silva, M. Henriques, *Candida glabrata*: a review of its features and resistance. *Eur J Clin Microbiol Infect Dis* 33, 673-688 (2014).

21. V. Krcmery, A. J. Barnes, Non-albicans Candida spp. causing fungaemia: pathogenicity and antifungal resistance. *J Hosp Infect* 50, 243-260 (2002).

22. Z. Weissman, D. Kornitzer, A family of Candida cell surface haem-binding proteins involved in haemin and haemoglobin-iron utilization. *Mol Microbiol* 53, 1209-1220 (2004).

23. R. Kaur, R. Domergue, M. L. Zupancic, B. P. Cormack, A yeast by any other name: *Candida glabrata* and its interaction with the host. *Curr Opin Microbiol* 8, 378-384 (2005).

24. Y. Hassan, S. Y. Chew, L. T. L. Than, *Candida glabrata*: Pathogenicity and Resistance Mechanisms for Adaptation and Survival. *J Fungi (Basel)* 7, (2021).

25. K. Kumar, F. Askari, M. S. Sahu, R. Kaur, *Candida glabrata*: A Lot More Than Meets the Eye. *Microorganisms* 7, (2019).

26. T. Widiasih Widiyanto, X. Chen, S. Iwatani, H. Chibana, S. Kajiwara, Role of major facilitator superfamily transporter Qdr2p in biofilm formation by *Candida glabrata*. *Mycoses* 62, 1154-1163 (2019).

27. M. Tscherner, T. Schwarzmüller, K. Kuchler, Pathogenesis and Antifungal Drug Resistance of the Human Fungal Pathogen *Candida glabrata*. *Pharmaceuticals* 4, 169-186 (2011).

28. S. Poláková, C. Blume, J. A. Zárate, M. Mentel, D. Jørck-Ramberg, J. Stenderup, J. Piskur, Formation of new chromosomes as a virulence mechanism in yeast *Candida glabrata*. *Proc Natl Acad Sci U S A* 106, 2688-2693 (2009).

29. B. Pathakumari, G. Liang, W. Liu, Immune defence to invasive fungal infections: A comprehensive review. *Biomed Pharmacother* 130, 110550 (2020).

30. J. L. Blanco, M. E. Garcia, Immune response to fungal infections. *Vet Immunol Immunopathol* 125, 47-70 (2008).

31. L. Romani, Immunity to fungal infections. *Nat Rev Immunol* 11, 275-288 (2011).

32. M. G. Netea, C. Van der Graaf, J. W. Van der Meer, B. J. Kullberg, Recognition of fungal pathogens by Toll-like receptors. *Eur J Clin Microbiol Infect Dis* 23, 672-676 (2004).

33. L. Kasper, K. Seider, B. Hube, Intracellular survival of *Candida glabrata* in macrophages: immune evasion and persistence. *FEMS Yeast Res* 15, fov042 (2015).

34. M. Riedelberger, P. Penninger, M. Tscherner, B. Hadriga, C. Brunnhofer, S. Jenull, A. Stoiber, C. Bourgeois, A. Petryshyn, W. Glaser, A. Limbeck, M. A. Lynes, G. Schabbauer, G. Weiss, K. Kuchler, Type I Interferons Ameliorate Zinc Intoxication of *Candida glabrata* by Macrophages and Promote Fungal Immune Evasion. *iScience* 23, 101121 (2020).

35. K. Y. Djoko, C. L. Ong, M. J. Walker, A. G. McEwan, The Role of Copper and Zinc Toxicity in Innate Immune Defense against Bacterial Pathogens. *J Biol Chem* 290, 18954-18961 (2015).

36. M. Galocha, P. Pais, M. Cavalheiro, D. Pereira, R. Viana, M. C. Teixeira, Divergent Approaches to Virulence in *C. albicans* and *C. glabrata*: Two Sides of the Same Coin. *Int J Mol Sci* 20, (2019).

37. L. Kasper *et al.*, Identification of *Candida glabrata* genes involved in pH modulation and modification of the phagosomal environment in macrophages. *PLoS One* 9, e96015 (2014).

38. A. C. Mesa-Arango, L. Scorzoni, O. Zaragoza, It only takes one to do many jobs: Amphotericin B as antifungal and immunomodulatory drug. *Front Microbiol* 3, 286 (2012).

39. J. Houšť, J. Spížek, V. Havlíček, Antifungal Drugs. *Metabolites* 10, (2020).

40. M. I. Morris, M. Villmann, Echinocandins in the management of invasive fungal infections, part 1. *Am J Health Syst Pharm* 63, 1693-1703 (2006).

41. O. Silakari, *Key heterocycle cores for designing multitargeting molecules.* (Elsevier, Amsterdam, Netherlands, 2018).

42. L. R. Peyton, S. Gallagher, M. Hashemzadeh, Triazole antifungals: a review. *Drugs Today (Barc)* 51, 705-718 (2015).

43. S. Campoy, J. L. Adrio, Antifungals. *Biochem Pharmacol* 133, 86-96 (2017).

44. S. Bhattacharya, B. D. Esquivel, T. C. C. P. White, Overexpression or Deletion of Ergosterol Biosynthesis Genes Alters Doubling Time, Response to Stress Agents, and Drug Susceptibility in *Saccharomyces cerevisiae. mBio* 9, (2018).

45. P. F. Watson, M. E. Rose, S. W. Ellis, H. England, S. L. Kelly, Defective sterol C5-6 desaturation and azole resistance: a new hypothesis for the mode of action of azole antifungals. *Biochem Biophys Res Commun* 164, 1170-1175 (1989).

46. S. L. Kelly, D. C. Lamb, A. J. Corran, B. C. Baldwin, D. E. Kelly, Mode of action and resistance to azole antifungals associated with the formation of 14 alpha-methylergosta-8,24(28)-dien-3 beta,6 alpha-diol. *Biochem Biophys Res Commun* 207, 910-915 (1995).

47. M. Kneale, J. S. Bartholomew, E. Davies, D. W. Denning, Global access to antifungal therapy and its variable cost. *J Antimicrob Chemother* 71, 3599-3606 (2016).

48. M. A. Ghannoum, L. B. Rice, Antifungal agents: mode of action, mechanisms of resistance, and correlation of these mechanisms with bacterial resistance. *Clin Microbiol Rev* 12, 501-517 (1999).

49. S. G. Whaley, P. D. Rogers, Azole Resistance in *Candida glabrata. Curr Infect Dis Rep* 18, 41 (2016).

50. B. D. Alexander *et al.*, Increasing echinocandin resistance in *Candida glabrata*: clinical failure correlates with presence of FKS mutations and elevated minimum inhibitory concentrations. *Clin Infect Dis* 56, 1724-1732 (2013).

51. S. Vallabhaneni, A. A. Cleveland, M. M. Farley, L. H. Harrison,W. Schaffner, Z. G. Beldavs, G. Derado, C. D. Pham, S. R. Lockhart, R. M. Smith, Epidemiology and Risk Factors for Echinocandin Nonsusceptible Candida glabrata Bloodstream Infections: Data From a Large Multisite Population-Based Candidemia Surveillance Program, 2008-2014. *Open Forum Infect Dis* 2, ofv163 (2015).

52. P. Pais, C. Pires, C. Costa, M. Okamoto, H. Chibana, M. C. Teixeira, Membrane Proteomics Analysis of the *Candida glabrata* Response to 5-Flucytosine: Unveiling the Role and Regulation of the Drug Efflux Transporters CgFlr1 and CgFlr2 . *Front Microbiol* 7, 2045 (2016).

53. L. A. Vale-Silva, D. Sanglard, Tipping the balance both ways: drug resistance and virulence in *Candida glabrata. FEMS Yeast Res* 15, fov025 (2015).

54. M. Zavrel, S. J. Hoot, T. C. White, Comparison of sterol import under aerobic and anaerobic conditions in three fungal species, *Candida albicans*, *Candida glabrata*, and *Saccharomyces cerevisiae. Eukaryot Cell* 12, 725-738 (2013).

55. M. Nagi, K. Tanabe, K. Ueno, H. Nakayama, T. Aoyama, H. Chibana, S. Yamagoe, T. Uneyama, T. Oura, H. Ohno, S. Kajiwara, Y. Miyazaki, The *Candida glabrata* sterol scavenging mechanism, mediated by the ATP-binding cassette transporter Aus1p, is regulated by iron limitation. *Mol Microbiol* 88, 371-381 (2013).

56. D. Sanglard, F. Ischer, D. Calabrese, P. A. Majcherczyk, J. C. P. Bille, The ATP binding cassette transporter gene CgCDR1 from *Candida glabrata* is involved in the resistance of clinical isolates to azole antifungal agents. *Antimicrob Agents Chemother* 43, 2753-2765 (1999).

57.   S. G. Whaley, Q. Zhang, K. E. Caudle, P. D. C. P. Rogers, Relative Contribution of the ABC Transporters Cdr1, Pdh1, and Snq2 to Azole Resistance in *Candida glabrata*. *Antimicrob Agents Chemother* 62, (2018).

58.   J. P. Vermitsky, K. D. Earhart, W. L. Smith, R. Homayouni, T. D. Edlind, P. D. Rogers, Pdr1 regulates multidrug resistance in *Candida glabrata*: gene disruption and genome-wide expression studies. *Mol Microbiol* 61, 704-722 (2006).

59.   H. F. Tsai, A. A. Krol, K. E. Sarti, J. E. C. P. Bennett, *Candida glabrata* PDR1, a transcriptional regulator of a pleiotropic drug resistance network, mediates azole resistance in clinical isolates and petite mutants. *Antimicrob Agents Chemother* 50, 1384-1392 (2006).

60.   K. R. Healey, C. Jimenez Ortigosa, E. Shor, D. S. Perlin, Genetic Drivers of Multidrug Resistance in *Candida glabrata*. *Front Microbiol* 7, 1995 (2016).

61.   J. E. Bennett, K. Izumikawa, K. A. C. P. Marr, Mechanism of increased fluconazole resistance in *Candida glabrata* during prophylaxis. *Antimicrob Agents Chemother* 48, 1773-1777 (2004).

62.   D. Allen, D. Wilson, R. Drew, J. Perfect, Azole antifungals: 35 years of invasive fungal infection management. *Expert Rev Anti Infect Ther* 13, 787-798 (2015).

63.   H. Zhao, D. J. Eide, Zap1p, a metalloregulatory protein involved in zinc-responsive transcriptional regulation in *Saccharomyces cerevisiae*. *Mol Cell Biol* 17, 5044-5052 (1997).

64.   C. Y. Wu, A. J. Bird, L. M. Chung, M. A. Newton, D. R. Winge, D. J. Eide, Differential control of Zap1-regulated genes in response to zinc deficiency in *Saccharomyces cerevisiae*. *BMC Genomics* 9, 370 (2008).

65.   C. J. Nobile, J. E. Nett, A. D. Hernday, O. R. Homann, J. Deneault, A. Nantel, D. R. Andes, A. D. Johnson, A. P. Mitchell, Biofilm matrix regulation by *Candida albicans* Zap1. *PLoS Biol* 7, e1000133 (2009).

66.   B. Böttcher, K. Palige, I. D. Jacobsen, B. Hube, S. Brunke, Csr1/Zap1 Maintains Zinc Homeostasis and Influences Virulence in *Candida dubliniensis* but Is Not Coupled to Morphogenesis. *Eukaryot Cell* 14, 661-670 (2015).

67.   R. Schneider, N. S. S. Fogaça, L. Kmetzsch, A. Schrank, M. H. Vainstein, C. C. Staats, Zap1 regulates zinc homeostasis and modulates virulence in *Cryptococcus gattii*. *PLoS One* 7, e43773 (2012).

68.   A. G. Frey, D. J. Eide, Roles of two activation domains in Zap1 in the response to zinc deficiency in *Saccharomyces cerevisiae*. *J Biol Chem* 286, 6844-6854 (2011).

69.   C. C. Staats, L. Kmetzsch, A. Schrank, M. H. Vainstein, Fungal zinc metabolism and its connections to virulence. *Front Cell Infect Microbiol* 3, 65 (2013).

70.   A. J. Bird, S. Labbé, The Zap1 transcriptional activator negatively regulates translation of the RTC4 mRNA through the use of alternative 5' transcript leaders. *Mol Microbiol* 106, 673-677 (2017).

71.   H. Zhao, E. Butler, J. Rodgers, T. Spizzo, S. Duesterhoeft, D. Eide Regulation of zinc homeostasis in yeast by binding of the ZAP1 transcriptional activator to zinc-responsive promoter elements. *J Biol Chem* 273, 28713-28720 (1998).

72.   T. J. Lyons, A. P. Gaschi, L. A. Gaither, D. Botstein, P. O. Brown, D. J. Eide ,Genome-wide characterization of the Zap1p zinc-responsive regulon in yeast. *Proc Natl Acad Sci U S A* 97, 7957-7962 (2000).

73.   G. M. Carman, G. S. Han, Regulation of phospholipid synthesis in *Saccharomyces cerevisiae* by zinc depletion. *Biochim Biophys Acta* 1771, 322-330 (2007).

74.   S. H. Han, G. S. Han, W. M. Iwanyshyn, G. M. Carman, Regulation of the PIS1-encoded phosphatidylinositol synthase in *Saccharomyces cerevisiae* by zinc. *J Biol Chem* 280, 29017-29024 (2005).

75.   W. M. Iwanyshyn, G. S. Han, G. M. Carman, Regulation of phospholipid synthesis in *Saccharomyces cerevisiae* by zinc. *J Biol Chem* 279, 21976-21983 (2004).

76.   C. Pimentel, C. Vicente, R. A. Menezes, S. Caetano, L. Carreto, C. Rodrigues-Pousada, The role of the Yap5 transcription factor in remodeling gene expression in response to Fe bioavailability. *PLoS One* 7, e37434 (2012).

77.   A. Gaspar-Cordeiro, S. Silva, M. Aguiar, C. Rodrigues-Pousada, H. Haas, L. M. P. Lima, C. Pimentel, A copper(II)-binding triazole derivative with ionophore properties is active against Candida spp. *J Biol Inorg Chem* 25, 1117-1128 (2020).

78.   T. R. Cabrito, M. C. Teixeira, A. Singh, R. Prasad, I. Sá-Correia, The yeast ABC transporter Pdr18 (ORF YNR070w) controls plasma membrane sterol composition, playing a role in multidrug resistance. *Biochem J* 440, 195-202 (2011).

79.   T. Jordá, S. Puig, Regulation of Ergosterol Biosynthesis in *Saccharomyces cerevisiae*. *Genes (Basel)* 11, (2020).

80.   S. Maesaki, P. Marichal, H. Vanden Bossche, D. Sanglard, S. Kohno, Rhodamine 6G efflux for the detection of CDR1-overexpressing azole-resistant *Candida albicans* strains. *J Antimicrob Chemother* 44, 27-31 (1999).

81.   G. Chua, Q. D. Morris, R. Spoko, M. D. Robinson, O. Ryan, E. T. Chan, B. J. Frey, B. J. Andrews, C. Boone, T. R. Hughes, Identifying transcription factor functions and targets by phenotypic activation. *Proc Natl Acad Sci U S A* 103, 12045-12050 (2006).

82.   W. Xu, N. V. Solis, R. L. Ehrlich, C. A. Woolford, S. G. Filler, A. P. Mitchell, Activation and alliance of regulatory pathways in *C. albicans* during mammalian infection. *PLoS Biol* 13, e1002076 (2015).

83.   J. P. Vermitsky, T. D. C. P. Edlind, Azole resistance in *Candida glabrata*: coordinate upregulation of multidrug transporters and evidence for a Pdr1-like transcription factor. *Antimicrob Agents Chemother* 48, 3773-3781 (2004).

84.   H. Elicharova, H. Sychrova, Fluconazole treatment hyperpolarizes the plasma membrane of Candida cells. *Med Mycol* 51, 785-794 (2013).

85.   D. Malavia, L. E. Lehtovirta-Morley, O. Alamir, E. Weiß, N. A. R. Gow, B. Hube, D. Wilson, Zinc Limitation Induces a Hyper-Adherent Goliath Phenotype in *Candida albicans*. *Front Microbiol* 8, 2238 (2017).

86.   L. A. Vale-Silva, B. Moeckli, R. Torelli, B. Posteraro, M. Sanguinetti, D. Sanglard, Upregulation of the Adhesin Gene EPA1 Mediated by PDR1 in *Candida glabrata* Leads to Enhanced Host Colonization. *mSphere* 1, (2016).

87.   S. Salari, N. Sadat Seddighi, P. Ghasemi Nejad Almani, Evaluation of biofilm formation ability in different Candida strains and anti-biofilm effects of Fe. *J Mycol Med* 28, 23-28 (2018).

88.   M. Marcet-Houben, T. Gabaldón, The tree versus the forest: the fungal tree of life and the topological diversity within the yeast phylome. *PLoS One* 4, e4357 (2009).

89.   B. E. Mansfield, H. N. Oltean, B. G. Oliver, S. J. Hoot, S. E. Leyde, L. Hedstrom, T. C. White, Azole drugs are imported by facilitated diffusion in *Candida albicans* and other pathogenic fungi. *PLoS Pathog* 6, e1001126 (2010).

90.   S. Khakhina, L. Simonicova, W. S. C. P. Moye-Rowley, Positive autoregulation and repression of transactivation are key regulatory features of the *Candida glabrata* Pdr1 transcription factor. *Mol Microbiol* 107, 747-764 (2018).

91.   J. K. Thakur *et al.*, A nuclear receptor-like pathway regulating multidrug resistance in fungi. *Nature* 452, 604-609 (2008).

92.   A. Soto-Cardalda, S. Fakas, F. Pascual, H. S. Choi, G. M. Carman, Phosphatidate phosphatase plays role in zinc-mediated regulation of phospholipid synthesis in yeast. *J Biol Chem* 287, 968-977 (2012).

93.   T. R. O'Meara, A. O. Veri, E. J. Polvi, X. Li, S. F. Valaei, S. Diezmann, L. E. Cowen, Mapping the Hsp90 Genetic Network Reveals Ergosterol Biosynthesis and Phosphatidylinositol-4-Kinase Signaling as Core Circuitry Governing Cellular Stress. *PLoS Genet* 12, e1006142 (2016).

94.   P. Bhakt, R. Shivarathri, D. K. Choudhary, S. Borah, R. Kaur, Fluconazole-induced actin cytoskeleton remodeling requires phosphatidylinositol 3-phosphate 5-kinase in the pathogenic yeast *Candida glabrata*. *Mol Microbiol* 110, 425-443 (2018).

95.   V. Ghugtyal, R. Garcia-Rodas, A. Seminara, S. Schaub, M. Bassilana, R. A. Arkowitz, Phosphatidylinositol-4-phosphate-dependent membrane traffic is critical for fungal filamentous growth. *Proc Natl Acad Sci U S A* 112, 8644-8649 (2015).

96.   M. Kodedová, H. C. P. Sychrová, Changes in the Sterol Composition of the Plasma Membrane Affect Membrane Potential, Salt Tolerance and the Activity of Multidrug Resistance Pumps in *Saccharomyces cerevisiae*. *PLoS One* 10, e0139306 (2015).

97.   J. Suchodolski, J. Muraszko, P. Bernat, A. C. P. Krasowska, A Crucial Role for Ergosterol in Plasma Membrane Composition, Localisation, and Activity of Cdr1p and H+-ATPase in *Candida albicans*. *Microorganisms* 7, (2019).

98.   L. J. Heung, Monocytes and the Host Response to Fungal Pathogens. *Front Cell Infect Microbiol* 10, 34 (2020).

99.   M. A. Moreno *et al.*, The regulation of zinc homeostasis by the ZafA transcriptional activator is essential for *Aspergillus fumigatus* virulence. *Mol Microbiol* 64, 1182-1197 (2007).

100.   A. Gaspar-Cordeiro *et al.*, Copper Acts Synergistically with Fluconazole in C*andida glabrata* by Compromising Drug Efflux, Sterol Metabolism, and Zinc Homeostasis. *bioRxiv*, 2021.2012.2022.473865 (2021).

101.   T. Schwarzmüller *et al.*, Systematic phenotyping of a large-scale *Candida glabrata* deletion collection reveals novel antifungal tolerance genes. *PLoS Pathog* **10**, e1004211 (2014).

102.   D. Davis, R. B. Wilson, A. P. Mitchell, RIM101-dependent and-independent pathways govern pH responses in *Candida albicans*. *Mol Cell Biol* **20**, 971-978 (2000).
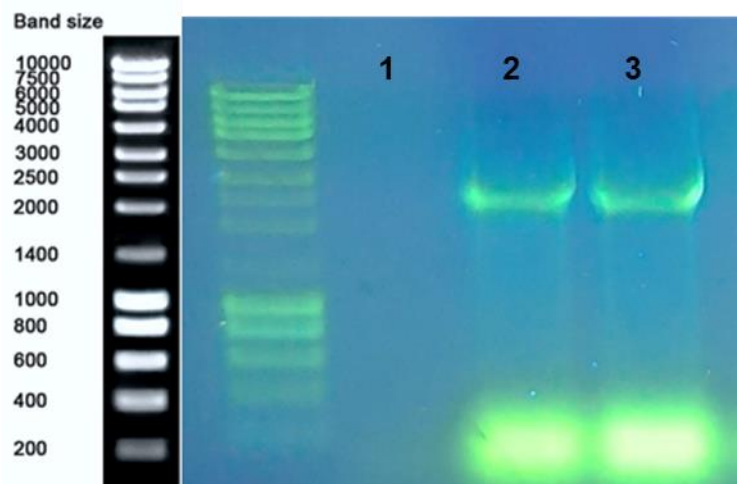
Figure 7.1: *C. glabrata ZAP1* **gene amplification confirmation.** Lane 2 and 3 positive (2533 bp), Lane 1 control no DNA.
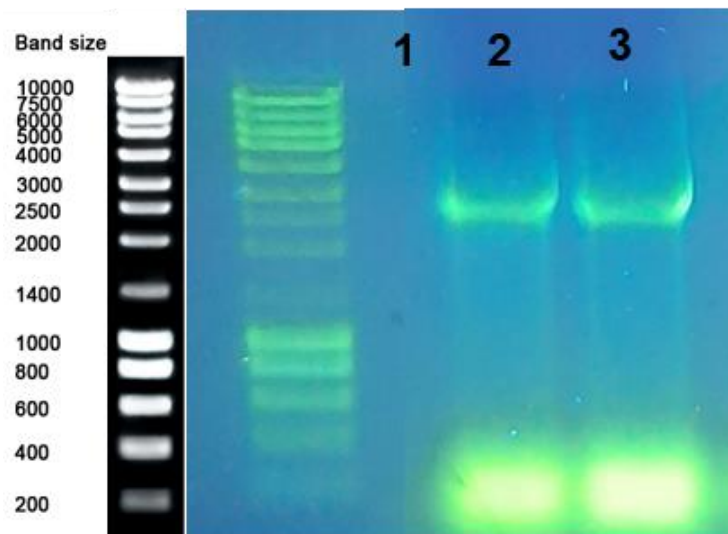

Figure 7.2: Confirmation of *ZAP1* **fragment integration in vector pCgACT-14.** Lane 2 and 3 positive (2888 bp), lane 1 control no DNA
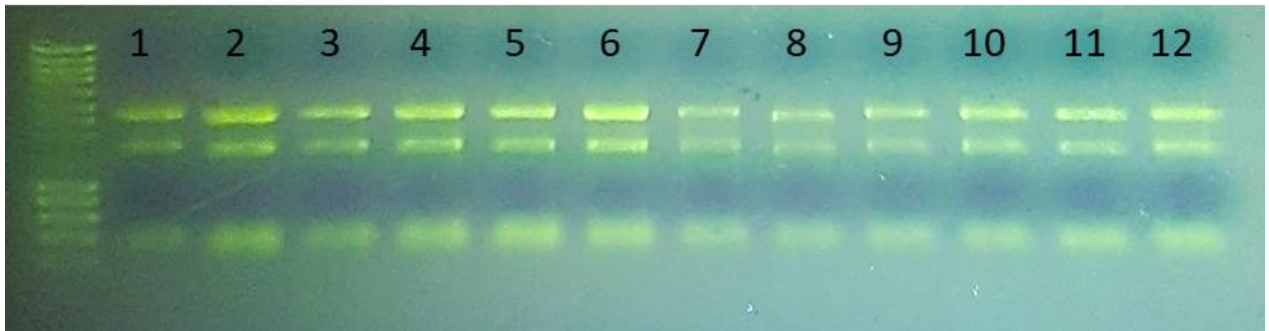
Figure 7.3: RNA integrity after RNA purification of *C. glabrata* WT and *CgΔzap1*. Lanes 1-3 and 4-6 are WT and *CgΔzap1* respectively, growth in SC medium. Lanes 7-9 and 10-12 are WT and *CgΔzap1* respectively, growth in SC without zinc medium. RNA in all samples is not degraded.
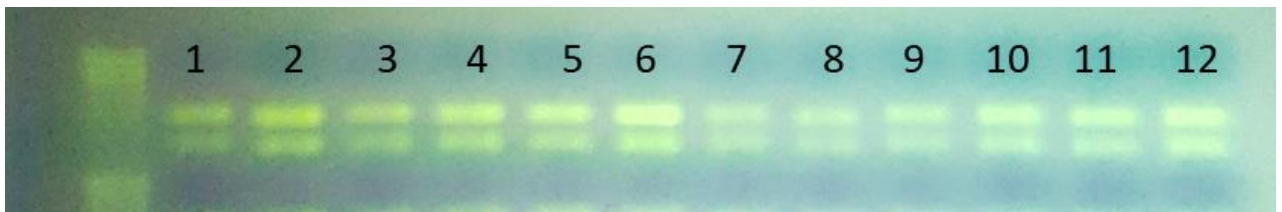

Figure 7.4: RNA integrity after DNase of *C. glabrata* WT and *CgΔzap1*. Lanes 1-3 and 4-6 are WT and *CgΔzap1* respectively, growth in SC medium. Lanes 7-9 and 10-12 are WT and *CgΔzap1* respectively, growth in SC without zinc medium. RNA in all samples is not degraded.

UNIVERSIDADE NOVA DE LISBOA

Zap1 is required for *Candida glabrata* response to fluconazole

Gonçalo Afonso

2021